

國立交通大學

電信工程研究所

碩 士 論 文

正交頻率多工訊號之峰均值降低之研究



Studies of Peak-to-Average Power Ratio Reduction for OFDM Signals

研 究 生：董原豪

指導教授：蘇育德 教授

中 華 民 國 九 十 九 年 七 月

正交頻率多工訊號之峰均值降低之研究

Studies of Peak-to-Average Power Ratio Reduction for OFDM Signals

研 究 生：董原豪

Student：Yuan-Hao Tung

指導教授：蘇育德

Advisor：Dr. Yu T. Su

國 立 交 通 大 學

電 信 工 程 研 究 所

碩 士 論 文

A Thesis

Submitted to Institute of Communication Engineering

College of Electrical and computer Engineering

National Chiao Tung University

in partial Fulfillment of the Requirements

for the Degree of

Master of science

in

Communication Engineering

July 2010

Hsinchu, Taiwan, Republic of China

中華民國九十九年七月

正交頻率多工訊號之峰均值降低之研究

學生:董原豪

指導教授:蘇育德 博士

國立交通大學電信工程研究所碩士班

摘 要

正交頻率多工(OFDM)系統可提供高資料傳輸量，但此系統會使時間訊號產生高峰均值(PAPR)的現象。而在這篇論文當中我們主要使用兩種方法，一種為裁剪法(Clipping)，一種為選擇性映射(Selective Mapping)。

傳統裁剪法，針對時間訊號的振幅做裁剪，而我們提出的裁剪法針對時間訊號實部跟虛部分開來裁剪；而在頻譜我們採用多種約束區域(Constraint set)，像是有界區域(Bounded Region)、主動式星座圖延展(Active Constellation Extension)、保留載波(Tone Reservation)，接著我們將整個問題公式化成線性規畫型式，再由已發展完善的線性規畫工具解出最佳被裁減的傳輸訊號。

另外，在探討選擇性映射時，會討論到旁解碼訊號(side information)的傳送，通常做法有兩種，我們個別對這兩種做法提出解決辦法。第一種是設計選擇性映射序列(Selective mapping sequences)，使得傳送端不用傳送旁解碼訊號，而接收機直接藉由判斷接收訊號的特徵判斷選擇性映射序列。而提出的設計能夠達到降低接收端偵測選擇性映射序列特徵(side information)的錯誤率，且同時維持此序列的降低峰均值能力。因為此序列的產生可以由群論找到極為簡單，耗費的記憶體也極少的方法，因此有實作上的貢獻；我們提出的另外一種方法是，將旁解碼訊號插入同一個被傳送的 OFDM Symbol，並且藉由調整旁解碼訊號的頻域訊號點而達到進一步降低峰均值以及降低旁解碼訊號偵測的錯誤率。

Studies of Peak-to-Average Power Ratio Reduction for OFDM Signals

Student : Yuan-Hao Tung

Advisor : Yu T. Su

Institute of Communications Engineering
National Chiao Tung University

Abstract

In this thesis we propose several approaches for reducing peak-to-average power ratio (PAPR) of orthogonal frequency division multiplexing (OFDM) signals.

The conventional clipping approach clips the magnitude of a time-domain OFDM waveform while leaving its phase intact. We present a novel time-domain clipping method with hybrid frequency domain constraint by independently clipping both real and imaginary parts of a complex time-domain OFDM waveform and using linear programming (LP) to obtain the optimal clipped signal.

Selective mapping (SLM) often requires that side information about the mapping sequence used be sent along with the desired data sequence. Maximum likelihood detection without side information is realized at the cost of much higher complexity. We proposed a novel SLM sequences design which enable a receiver to use a simple detector without side information, leading to bandwidth efficiency and capacity improvement. The proposed design also has the advantages of simple encoding implementation and low memory requirement.

When SLM side information is needed for signal detection, it is often protected with a low rate forward error-correcting code. We propose an SLM scheme with embedded side information. Active constellation extension (ACE) and projection onto convex set (POCS) techniques are used to adjust side information for both reducing PAPR and achieving better SLM index detection probability.

誌 謝

人生的第一個求學階段(小學、國中、高中、大學、研究所)在交通大學電信工程研究所做一個總結，感謝學校和系上給予的所有資源，不僅讓我在書本中開眼界，也能到美國嘗試交換學生的經驗，讓我的求學生涯與眾不同。在許許多多要感謝的教授當中，我特別感謝我的指導教授蘇育德博士，因為他的指導我的論文才能夠這麼順利的完成；除了專業知識外，在碩士班每周一次的報告當中加入實驗室成員的生活經驗分享，並且分享老師個人的人生經驗，讓我在做人處事方面能夠更加成熟、更加全面。

我還要感謝實驗室的林坤昌學長，在我大學部專題以及碩士班兩年在研究方面指導我，給予我很多很好的建議、觀念與經驗分享，幫助我的論文完成；除了研究之外，平常跟學長日常生活相處當中也獲得不少做人處事的觀念及態度。另外也感謝實驗室所有的學長姐(博士班的學長們、96級的碩班學長姐)給予的指導，感謝實驗室97級同學這兩年一起同甘共苦，以及98級學弟妹這一年的陪伴，希望大家在之後人生的路上都順遂。還要再感謝實驗室的助理(淑琪姐、昱岑姐)，幫忙實驗室處理大大小小的事情，幫忙我處理去國外會議的報帳問題。謝謝你們。

感謝我的家人，一直以來不求回報的付出，並且在生活跟心靈上的支持，讓我無後顧之憂的往前衝刺往目標邁進。今天我以我很棒的家庭為榮，希望之後我的家人們能以我為榮。

最後，感謝每一個幫助過我的人、一起揮灑過汗水的夥伴、一起歡笑的朋友，感謝你！

董原豪謹誌 于新竹國立交通大學

Contents

Contents	iv
List of Figures	vi
List of Tables	ix
1 Introduction	1
2 Orthogonal Frequency Division Multiplexing and Peak-to-Average Power Ratio	5
3 Non-linear clipping with hybrid frequency domain constraints	10
3.1 Background	10
3.2 PAPR and Available Subcarriers in OFDM Systems	11
3.3 Nonlinear Clipping as an Optimization Problem	12
3.3.1 Clipping as Multiple Constraints	13
3.3.2 Bounded Constellation Errors	15
3.4 Simulation Results	18
3.5 Chapter Summary	23
4 Selective Mapping without Side Information	24
4.1 Background	24
4.2 System Model	25
4.3 Sequence design criteria	29

4.4	A Review on Group Theory	30
4.5	Proposed SLM Sequence Design	31
4.6	Low Complexity SLM Encoder	35
4.7	Simulation Results	37
4.8	Chapter Summary	42
5	Selective Mapping with Embedded Side Information	43
5.1	System Model	43
5.2	Encoding Side Information and Insertion	45
5.2.1	Insertion of the Side Information	45
5.2.2	Estimation of Side Information	45
5.2.3	Encoding Scheme of SI	46
5.3	Side Information Adjustment Algorithm	47
5.3.1	Problem Formulation	47
5.3.2	Active Constellation Extension for SI Adjustment	48
5.3.3	Projection onto Complex Set for SI Adjustment	51
5.4	Numerical Results	53
5.5	Chapter Summary	56
6	Conclusion	58
6.1	Summary of Contributions	58
6.2	Some Future Works	59
	Bibliography	63

List of Figures

2.1	Block diagram of OFDM system.	5
2.2	Bandwidth utilization of OFDM system.	6
2.3	Time domain signal of a 16-channel OFDM signal, modulated with the same phase for all sub-channels.	7
2.4	input/output characteristic curve of a power amplifier.	8
3.1	Conventional clipping block diagram.	10
3.2	Block diagram of proposed clipping approach.	11
3.3	The time domain clipping rule.	13
3.4	Constellation error constraints for 16-QAM. Those colored area of internal points are bounded region and those for external points are extended region.	15
3.5	Original time-domain signal with PAPR=9.6448 dB.	19
3.6	Clipped time-domain signal with PAPR=5.9015 dB.	20
3.7	Constellation of distorted frequency-domain signal achieving 3.7433 dB PAPR reduction.	20
3.8	Phase difference and amplitude trajectories of a typical time-domain sequence before and after nonlinear clipping.	21
3.9	Effective PAPR gain for 16-QAM 256-carrier OFDM symbol with L=4 over-sampling for $\delta = 0.05d_{min}$, $\delta = 0.1d_{min}$, ACE, RCFBD, and separated coordinate PAPR.	22
3.10	BER of a 16-QAM and 256-carrier OFDM system.	22

4.1	Original SLM encoder.	25
4.2	SLM decoder proposed by Tellambura and Jayalath in [10].	26
4.3	Distribution of generated element g_k on unit circle.	33
4.4	Block diagram of low complexity SLM encoder.	35
4.5	Block diagram of modified low complexity SLM encoder.	37
4.6	CCDF plot of PAPR performance of random sequences, chaotic sequences, and proposed sequences design.	38
4.7	Probability of sequence index detection failure under frequency selective channel.	39
4.8	Euclidean distance of random sequences, chaotic sequences, and proposed sequence design.	39
4.9	Probability of sequence index detection failure of proposed sequences and Alsusa and Yang sequences under frequency selective channel.	40
4.10	CCDF of PAPR performance of original OFDM symbol, low complexity SLM encoder, and original SLM.	40
5.1	Bandwidth utilization of proposed scheme.	43
5.2	Original SLM encoder with embedded SI.	44
5.3	Extended region of QPSK denoted as F	48
5.4	Amplitude modulation for POCS algorithm.	51
5.5	Location of modified SI symbol using active constellation extension (ACE) algorithm.	54
5.6	Location of modified SI symbol using projection onto complex set (POCS) algorithm.	54
5.7	Key error rate for ACE and POCS schemes.	55
5.8	CCDF of PAPR of original SLM, SLM embedded SI, and SLM with mod- ified SI (ACE).	55

5.9 CCDF of PAPR of original SLM, SLM embedded SI, and SLM with modified SI (POCS). 56



List of Tables

5.1	Active constellation extension with smart gradient projection algorithm.	50
5.2	Projection onto Complex Set algorithm.	52



Chapter 1

Introduction

Recent developments in digital content have made the demand on video stream from youtube and editing documents through a remote server basic functional requirements for an intelligent portable handset. Orthogonal frequency division multiplexing (OFDM) is a well known technique for high mobility wireless transmissions. It modulates demultiplexed data streams on a large number of orthogonal sub-carriers with minimum spacing, converting a wideband waveform into parallel narrowband signals. The primary advantage of OFDM over single-carrier schemes is its ability to cope with severe channel conditions without the need of complex equalization.

However, OFDM waveforms often have high amplitude fluctuations and result in large peak-to-average power ratio (PAPR). As the digital-to-analog (DA) converter and power amplifier (PA) in a transmitter and the analog-to-digital (AD) converter used in the receiving end have limited linear operating range, high PAPRs would lead to various nonlinear distortions and growth of out-of-band spectrum. Significant input back-off is thus called for to reduce such undesired effects at the cost of low power efficiency.

Intensive research efforts have been devoted to solve the high PAPR/low power efficiency problem. The proposed solutions can be classified into three categories. The first category is coding scheme [1] [2]. A subset of signal with lower PAPR is transmitted instead of using the whole signal space, and a pre-defined mapping rule between information bit stream and signal subset has to be set up. Besides, low density parity

check code (LDPC) and turbo code can be used for PAPR reduction, in which several encoders with equal code rate are adopted.

The second category includes several signal distortion schemes which modify (distort) both time domain and frequency domain signal to reduce PAPR. The recursive clipping and filtering (RCF) [7] method clips time domain signal and filters out frequency side-lobes iteratively. Active constellation extension (ACE) [4] clips signal in time domain and forces frequency domain components to stay within an extended region so that no BER degradation will incur. The tone reservation (TR) approach [6][8] adds dummy complex values on those pre-defined reserved tones to reduce PAPR. Tone injection (TI) [1], on the other hand, adjusts frequency domain signal by choosing transmitted signal from alternative signal points to reduce time domain peaks. Usually, a convex optimization process is involved in these schemes and several sub-optimal approaches, greedy and CE, have been proposed to solve the associated optimization problem.

The last category involves different signal scrambling schemes. The so-called selective mapping (SLM) [9] method scrambles signal with several pre-defined scrambling sequences and selects the one with lowest PAPR value to transmit. Interleaving [3] rearrange frequency domain data vector in several pre-defined orders and chooses the one with lowest PAPR to transmit. Partial transmit sequence (PTS) [1] is a reduced-complexity SLM that frequency domain signal is divided into several blocks and each block is scrambled by the same complex value. Also, PTS encoder selects the one with lowest PAPR to transmit. These schemes produce many alternative frequency domain expression as candidates for one OFDM symbol, and transmitter chooses the one with minimum PAPR to transmit. Although, these schemes reduce PAPR significantly, side information is needed to have perfect de-scramble at the receiver. The options of transmission of side information can be further divided into two subcategories. The first subcategory suggests that scrambling sequence or re-ordering indices shall be greatly distinguishable by decoder without transmitting side information. The second one trans-

mits side information within the same OFDM symbol which the decoder should detect before using it to decode data symbol.

In this thesis, we propose three new PAPR reduction approaches that belong to the latter two categories. We first investigate a nonlinear clipping-related method. Conventional clipping approach only clips the magnitude of time domain signal and leaves the phase time domain signal unchanged. Some improved versions further set up boundaries for containing the frequency domain error vector to maintain bit-error-rate performance, and others leave in-band data with no limitation. But all the schemes strictly require that out-of-band sub-carriers stay zero. We propose a novel clipping method which clips time domain signal in real and imaginary parts separately. The proposed approach obtains the optimal clipped signal by solving a linear programming (LP) problem involves bounded region (BR), active constellation extension (ACE) and tone reservation (TR) constraints as well as a time domain clipping rule.

Our second and third contributions have to do with the SLM approach. A suitable SLM method is often capable of giving very impressive PAPR reduction performance and can be implemented in a parallel fashion to reduce the processing time. There are several major SLM-related design issues, however. The first issue is the complexities of encoder and decoder, the second one is about the transmission of side information between transmitter and receiver while the third critical issue is the design of good SLM sequences where the “goodness” is measured by the corresponding optimal PAPR reduction performance and blind detection probability.

We begin with a study on the SLM sequences which are designed for blind (no side information) detection. Many known SLM sequences like those generated by Hadamard matrix or Riemann matrix and chaotic sequences are non-constant modulus sequences which have the undesired noise enhancement effect at the receiving side. Constant modulus polyphase sequences such as random phase sequences and Chu sequences are used for SLM application before. Jayalath and Tellambura proposed a blind SLM decoding

method which simultaneously estimate the SLM sequence used and the transmitted data based on the generalized Euclidean distance. We propose a new class of polyphase SLM sequences which have maximum generalized Euclidean distance between two arbitrary combined data and SLM sequences. Our method results in improved blind detection performance and can be easily implemented with less memory requirement.

Our final contribution is concerned about side information transmission for the SLM approach. There are two methods for sending the SLM sequence information to the receiver. The first method hides the side information in sequence in such a way that it could be blindly detected. The alternative method transmits the side information within the same OFDM symbol. The receiver shall first detect side information and then decode the OFDM message accordingly. We provide another solution to insert side information in the transmitted OFDM symbol. The proposed scheme contains two stage. First stage is SLM encoder which selects OFDM symbol, scrambled by SLM sequence and carried side information, with lowest PAPR to transmit. A clipping stage is cascaded to further adjust side information to reduce PAPR. For different side information constraint sets, steepest descent projection (SDP) algorithm for ACE constraint and projection onto convex set (POCS) for circular constraint are adopted. The comparison for these two approaches are provided.

The rest of the thesis is organized as follow. The ensuing chapter provides a general description of OFDM systems and the associated PAPR problem. Both conventional clipping and the proposed nonlinear clipping algorithms and some simulated PAPR curves and BER performance are presented in Chapter 3. In Chapter 4, we introduce the SLM scheme and a blind sequence decoder. After a brief review on related group theory we propose a novel SLM sequence design and give some simulation results. In Chapter 5, we present a scheme which uses SLM in conjunction with nonlinear clipping. We provide some concluding remarks and suggest several topics for future studies.

Chapter 2

Orthogonal Frequency Division Multiplexing and Peak-to-Average Power Ratio

The basic idea of orthogonal frequency division multiplexing (OFDM) is to split a high-rate data stream into several lower rate streams which are transmitted simultaneously over a number of sub-channels. Because the symbol duration of lower rate streams increases, the relative amount of dispersion caused by multi-path delay spread is decreased. Inter-symbol Interference (ISI) can be eliminated by introducing the guard time, and cyclic Prefix (CP) is also introduced to avoid inter-carrier interference (ICI).

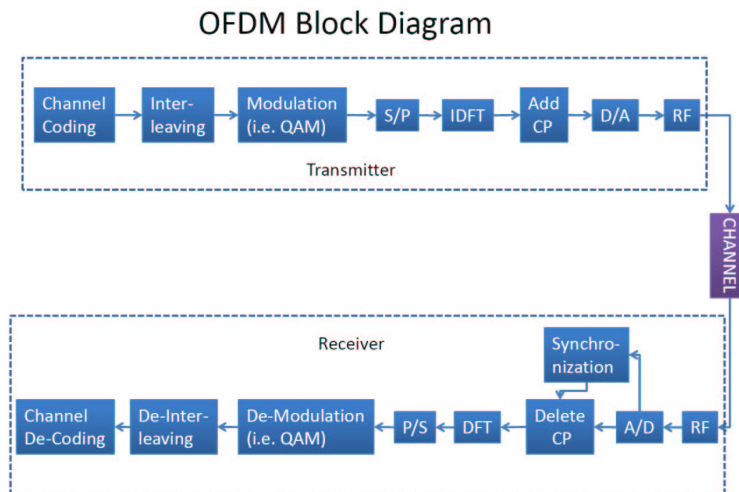


Figure 2.1: Block diagram of OFDM system.

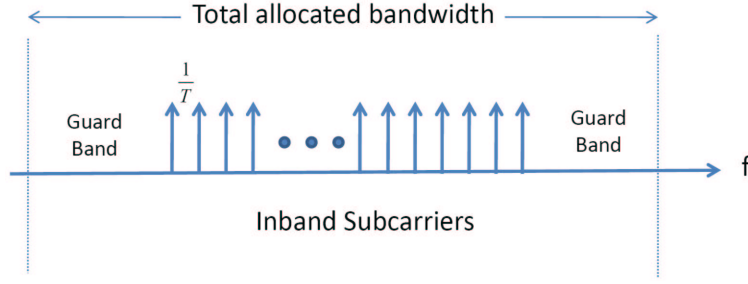


Figure 2.2: Bandwidth utilization of OFDM system.

Basic OFDM transceiver block diagram is provided above. Information bit stream is firstly encoded by channel coding (i.e. BCH code, convolutional code, or turbo code) and then is passed through an inter-leaver to alleviate channel deep fade effect. Serial-to-parallel (S/P) is used to connect modulation block output port and fast fourier transform block input port. The relation between discrete time and frequency OFDM signal is defined as

$$s[n] = \sum_{k=0}^{N-1} d[k] \exp\left(\frac{j2\pi nk}{N}\right) \quad (2.1)$$

is in fact an inverse discrete fourier transform (IDFT). In practice, this transform can be implemented efficiently by the inverse fast fourier transform (IFFT). Using radix-2 algorithm, complexity of IFFT can be further reduce to $O(N \log(N))$. After time domain signal $s[n]$ is obtained from IFFT block, CP shall be added and then digital-to-analog (D/A) or pulse shaping is involved to transfer signal from discrete to analog. Radio frequency block consists of up-converter, low noise amplifier (LNA), and antenna. This is structure of transmitter, and receiver is in a reverse fashion and each block has inverse function of the corresponding one in transmitter. The discrete fourier transform (DFT) is define as

$$d[k] = \sum_{n=0}^{N-1} s[n] \exp\left(\frac{-j2\pi nk}{N}\right) \quad (2.2)$$

The sub-carrier spacing is $\frac{1}{T}$ where T is OFDM symbol duration without CP. The OFDM spectrum fulfills Nyquist criterium by having maximum number of carriers correspond to zero crossing of all the others. Hence, OFDM has best spectral efficiency.

In addition, guard band is introduced and forced to be zero to mitigate adjacent band interference.

An OFDM signal consists of a sum of sub-carriers that are modulated by phase shift keying (PSK) or quadrature amplitude modulation (QAM) which can have a large peak-to-average power ratio when added up coherently. When N signals are added with the same phase, they produce a peak power that is N times the average power. This effect is illustrate in Fig. 2.3. For this example, the peak power is 64 times the average value.

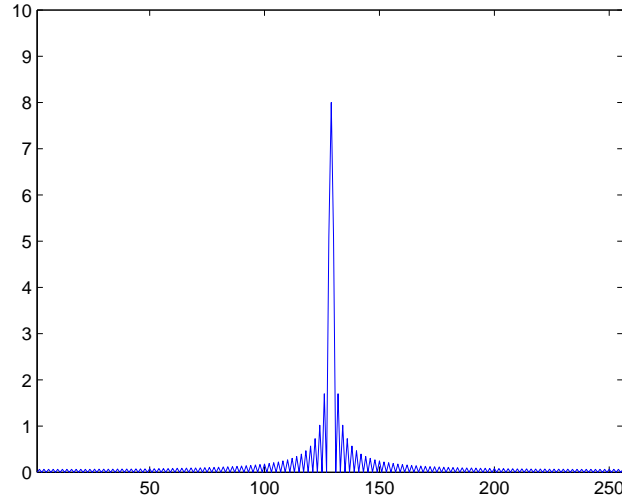


Figure 2.3: Time domain signal of a 16-channel OFDM signal, modulated with the same phase for all sub-channels.

A large peak-to-average power ratio brings disadvantages like an increased complexity of the analog-to-digital and digital-to-analog converters and a reduced power efficiency of the RF power amplifier. We observe the input/output characteristic curve of a power amplifier (Fig. 2.4), large peak forces signal fall into saturation region which will cause in-band signal distortion and side-lobe regrowth.

Back-off is needed that operation point is moved toward origin to avoid signal from clipping, thus power efficiency decreases proportionally with back-off range. Also, dis-

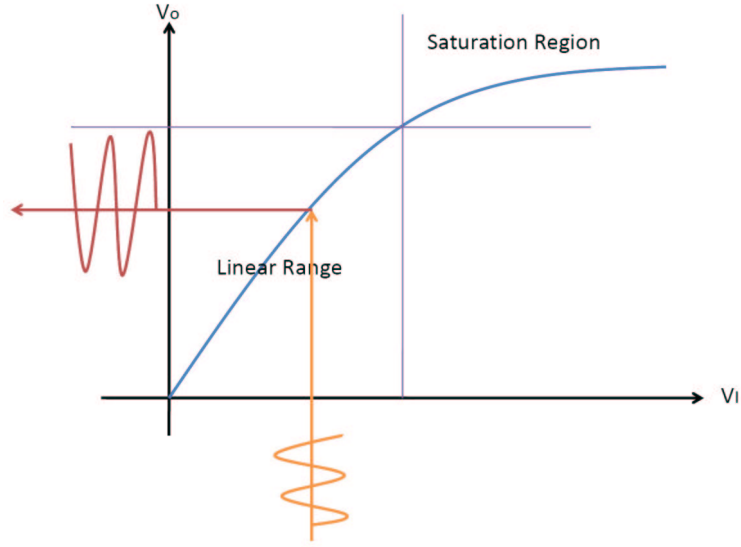


Figure 2.4: input/output characteristic curve of a power amplifier.

tortion will cause bit-error rate (BER) performance degradation and side-lobe regrowth will violate the frequency mask defined by communication specification. After knowing the drawback of PAPR, the measurement of PAPR should be mentioned.

Complementary cumulative distribution function (CCDF) is the measurement of PAPR which means the show up probability of the OFDM symbol of such PAPR value. Since symbols in frequency domain are independent, the time domain samples are uncorrelated with complex gaussian distribution. And the magnitude can be model as exponential distribution or Rayleigh distribution, thus the CCDF of PAPR can be calculated easily. When the number of sub-carriers N is relatively small the CCDF expression of the PAPR of OFDM signals can be written as

$$Prob\{CCDF > \gamma\} = 1 = (1 - e^{-\gamma})^N \quad (2.3)$$

However, above equation does not fit for OFDM system with large number of sub-carriers N . An alternative representation is written as

$$Prob\{CCDF > \gamma\} = 1 = (1 - e^{-\gamma})^{2.8N} \quad (2.4)$$

CCDF expression is used in the simulation results section in the following several chap-

ters to evaluate the performance of each proposed approach. Also, an over-sampling factor $L \geq 4$ is needed to ensure a negligible approximation error if the discrete PAPR analysis is to be used to approximate analog waveforms.

In the following three chapters, we proposed three different PAPR reduction approaches, non-linear clipping, selective mapping sequences design, and selective mapping with embedded side information. The first one is in signal distortion category and the second and third ones are in symbol scrambling category.

Notation: j denotes $\sqrt{-1}$. $(\cdot)^T$ and $(\cdot)^H$ represent transpose and Hermitian operations. $Re(\cdot)$ and $Im(\cdot)$ stand for the real and imaginary part of a complex signal. $|\cdot|$, $\|a\|$, and $\|\cdot\|_2$ represent cardinality, absolute value of a , and 2-norm, respectively. \otimes and \odot stand for the kronecker product, element-wise multiplication. $PAPR(\mathbf{x})$ gives PAPR value of the time domain OFDM symbol \mathbf{x} and $D(\mathbf{x}_1, \mathbf{x}_2)$ is the pairwise distance function of sequence \mathbf{x}_1 and \mathbf{x}_2 . $proj\{a, A\}$ projects point a onto the nearest point in set A .



Chapter 3

Non-linear clipping with hybrid frequency domain constraints

3.1 Background

The simplest approach to cope with PAPR is to clip those high magnitude peaks. The nonlinear clipping operation induces extra sidelobe spectrum which is suppressed by filtering the clipped waveform. Shown in Fig. 3.1 is a typical clip-and-filter PAPR reduction system. Significant signal distortion may be introduced as a result.

Conventional clipping methods clips time domain signal in magnitude and filter out out-of-band components and leave in-band components intact. As in-band distortion causes bit-error rate (BER) degradation, it is necessary to impose frequency domain constraints to limit the distortion. Active constellation extension (ACE) [4] approach

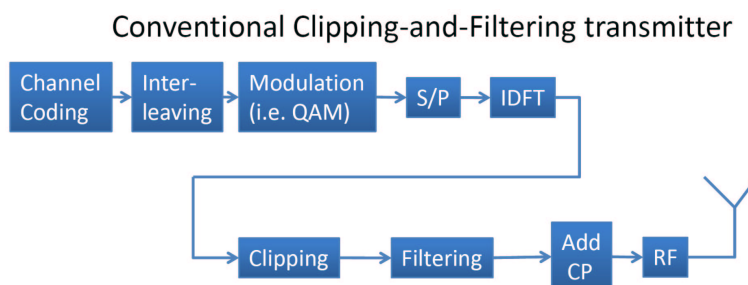


Figure 3.1: Conventional clipping block diagram.

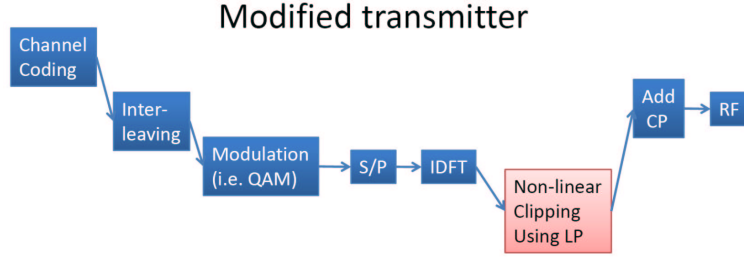


Figure 3.2: Block diagram of proposed clipping approach.

allows external constellation points to go outward to reduce peak magnitude. Bounded region (BR) [5] method let every constellation points to move within certain area inside decision region to reduce PAPR. Tone reservation (TR) [8] reserves several unused pilots to carry dummy complex values with no constraint to cancel peaks.

The proposed approach (see Fig. 3.2) is similar to the conventional clipping approach in which the clipping operation is performed on the complex time-domain data vector. Unlike conventional approaches, we clip the real and imaginary parts of the time domain signal separately. BR, ACE, TR constraints are adopted at the same time to have the largest frequency domain feasible set. We formulate this problem into linear programming (LP) standard form and use well-developed LP tools to solve for optimal clipped OFDM symbol.

The rest of the chapter is organized as follows: In Section II, we introduce basic definitions of a typical OFDM system. Section III presents the proposed approach formulated as an optimization problem and the following section provides some simulation results. Some concluding remarks are given in Section V.

3.2 PAPR and Available Subcarriers in OFDM Systems

An N -channel OFDM symbol consists of N sub-carriers with frequency f_k , $k = 0, 1, 2, \dots, N-1$ and frequency spacing $\Delta f = \frac{1}{T}$, where T is the symbol duration without the cyclic prefix (CP). Each subcarrier is carried an M -QAM data symbol and such frequency

domain OFDM symbol can be expressed as $\mathbf{X} = [X(0), X(1), \dots, X(N-1)]^T$.

An over-sampling factor $L \geq 4$ is needed to ensure a negligible approximation error if the discrete PAPR analysis is to be used to approximate analog waveforms. Denote the zero-padded frequency domain symbol by $\mathbf{X} = [X(0), X(1), \dots, X(N-1), 0, \dots, 0]^T$, which is an $NL \times 1$ vector. Then the over-sampled time domain signal is given by

$$x[n] = \frac{1}{\sqrt{NL}} \sum_{k=0}^{NL-1} X_k e^{j\frac{2\pi kn}{NL}}, \quad 0 \leq n \leq NL-1 \quad (3.1)$$

The PAPR of an OFDM symbol is defined as

$$PAPR(\mathbf{x}) = \frac{\max_{0 \leq n \leq NL-1} |x[n]|^2}{E[|x[n]|^2]} \quad (3.2)$$

where $\mathbf{x} = \mathbf{Q}\mathbf{X}$ and \mathbf{Q} is an $(NL \times NL)$ inverse discrete Fourier transform (IDFT) matrix.

Let the set of subcarriers that serves encoded data be denoted by Ω_d , where $|\Omega_d| = N_d$ and $|\cdot|$ denotes the cardinality. The subcarrier set in which free pilots are placed is Ω_{TR} , where $|\Omega_{TR}| = N_{TR}$. The subcarriers $f_k \in \Omega_d \cup \Omega_{TR}$ and $|\Omega_d \cup \Omega_{TR}| = N_t$ are called in-band subcarriers. The remaining subcarriers are used as guardband. The time domain representation of the transmitted frequency vector $\mathbf{X} = [X(k)]^T$, $k \in \Omega_d \cup \Omega_{TR}$, is given by $\mathbf{x} = \tilde{\mathbf{Q}}\mathbf{X}$, where $\tilde{\mathbf{Q}} =$

$$\frac{1}{\sqrt{NL}} \begin{pmatrix} 1 & 1 & \dots & 1 \\ e^{j\frac{2\pi f_1}{NL}} & e^{j\frac{2\pi f_2}{NL}} & \dots & e^{j\frac{2\pi f_{N_t}}{NL}} \\ \vdots & \vdots & \ddots & \vdots \\ e^{j\frac{2\pi f_1(NL-1)}{NL}} & e^{j\frac{2\pi f_2(NL-1)}{NL}} & \dots & e^{j\frac{2\pi f_{N_t}(NL-1)}{NL}} \end{pmatrix} \quad (3.3)$$

$f_1, \dots, f_{N_t} \in \Omega_d \cup \Omega_{TR}$.

The real and imaginary parts of the over-sampling IDFT matrix are denoted by $\mathbf{Q}_C = \text{Re}(\tilde{\mathbf{Q}})$, an $(NL \times N_t)$ matrix, and $\mathbf{Q}_S = \text{Im}(\tilde{\mathbf{Q}})$ which is an $(NL \times N_t)$ matrix.

3.3 Nonlinear Clipping as an Optimization Problem

The idea of our nonlinear clipping technique is to find an optimal clipping threshold and error vector such that all real and imaginary parts of the clipped time-domain

signal samples be smaller than the threshold. It is also required that this threshold be minimized while frequency domain error vector satisfies all the frequency domain constraints.

We add to the original vector \mathbf{x} a time-domain error vector $\mathbf{e} = [e_1, e_2, \dots, e_{NL}]$ to minimize the peaks in both I- and Q-channels. \mathbf{e} is to be determined at the transmit site. There will be no need to send any side information or modify the receiver structure. The DFT of \mathbf{e} , i.e., the frequency domain error vector is defined as $\mathbf{E} = [\underbrace{0, \dots, 0}_{\frac{(N-N_t)}{2}}, E_1, E_2, \dots, E_{N_t}, \underbrace{0, \dots, 0}_{N(L-\frac{1}{2})-\frac{N_t}{2}}] = \text{DFT}[\mathbf{e}]$. \mathbf{e} and \mathbf{E} are introduced to reduce PAPR. Moreover, there are free pilots (reserved tones) whose locations form a set which is disjoint to data subcarrier set.

3.3.1 Clipping as Multiple Constraints

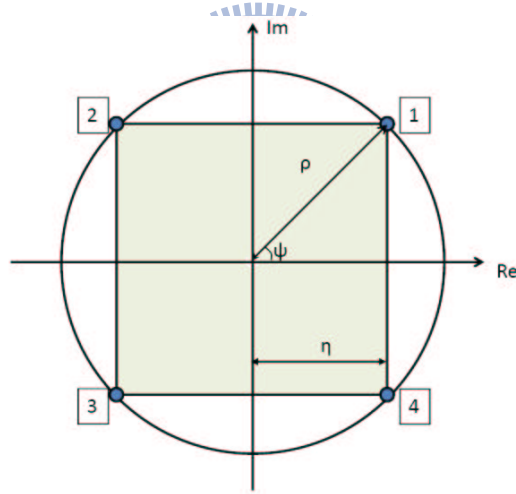


Figure 3.3: The time domain clipping rule.

Conventional clipping techniques [5], [7] clip only those peaks which exceed the clipping threshold while keeping the corresponding phase intact. In contrast, the proposed algorithm clips the real and imaginary parts of the samples separately and thus brings in one more degree of freedom. This extra dimension also manifests in the polar coordinate in which, unlike the conventional approach, the phases $\tan^{-1} \left[\frac{\text{Im}(x_i)}{\text{Re}(x_i)} \right]$ of the clipped

samples are allowed and likely to be different after clipping. Fig. 3.3 shows that our clipping rule confines all complex samples to stay inside the square with side length 2η , i.e., the magnitudes of their real and imaginary parts cannot be greater than η . Given an error vector \mathbf{e} and the original time-domain vector \mathbf{x} , the clipped samples becomes $\tilde{\mathbf{x}} = \mathbf{x} + \mathbf{e}$ which should satisfy the constraints:

$$\tilde{x} = \begin{cases} \|Re(\mathbf{x}) + Re(\mathbf{e})\|_{\infty} \leq \eta \\ \|Im(\mathbf{x}) + Im(\mathbf{e})\|_{\infty} \leq \eta \end{cases} \quad (3.4)$$

where $\|\cdot\|_{\infty}$ stands for infinite norm. The above discussion implies that our approach can be formulated as the following constrained linear programming (CLP) problem

$$\begin{aligned} & \min \eta \\ & \text{subject to :} \quad Re(\mathbf{x} + \mathbf{e}) \preceq \eta \mathbf{1} \\ & \quad \quad \quad Im(\mathbf{x} + \mathbf{e}) \preceq \eta \mathbf{1} \\ & \quad \quad \quad -Re(\mathbf{x} + \mathbf{e}) \preceq \eta \mathbf{1} \\ & \quad \quad \quad -Im(\mathbf{x} + \mathbf{e}) \preceq \eta \mathbf{1} \\ & \text{in variables :} \quad \mathbf{e} \in \mathbb{C}^{NL} \end{aligned} \quad (3.5)$$

where $\mathbf{1}$ stands for an $LN \times 1$ vector and \preceq denotes componentwise inequality in \mathbb{R}^m : $u \preceq v$ means $u_i \leq v_i$ for $i = 1, \dots, m$.

When the signal is clipped in time domain, distortions (sidelobe re-growth) are also generated in frequency domain. The resulting distortion is proportional to the magnitude of error vector \mathbf{e} . Although time domain clipping can achieve good PAPR performance, the frequency domain distortion might be very high, leading to BER degradation. To maintain acceptable BER performance, we need also to enforce constraints on the frequency domain error vector.

The difference between error vector magnitude (EVM) and constellation error is that EVM is based on 2-norm metric and there might be large errors in some coordinates

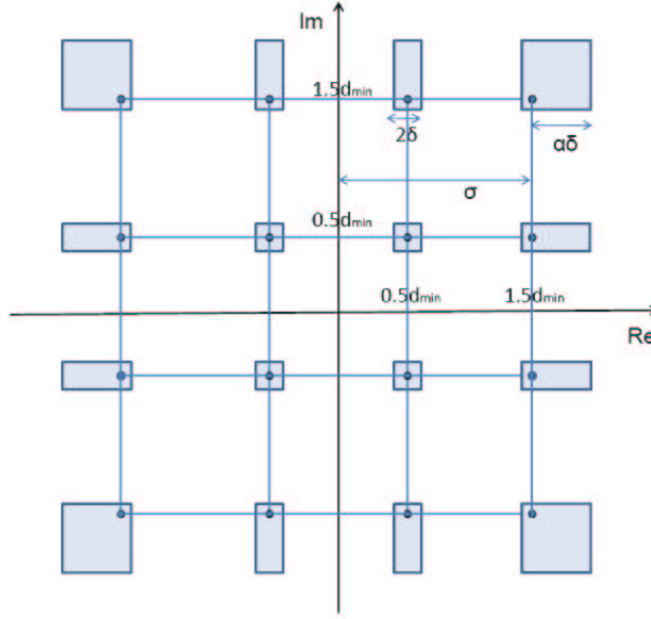


Figure 3.4: Constellation error constraints for 16-QAM. Those colored area of internal points are bounded region and those for external points are extended region.

without violating the error magnitude constraint but the constellation error measure ensures all coordinates of the error vector be within the constraint.

We use the constellation error to place constraints on the frequency-domain error vector \mathbf{E} to further reduce the feasible set of optimal clipping threshold η . Here, we limit the real and imaginary parts of E_i , the i th component of \mathbf{E} , to stay in the bounded region and extended region (see Fig. 3.4). The constellation error constraint is further elaborated and a new CLP formulation in the next subsection.

3.3.2 Bounded Constellation Errors

Recall that $\mathbf{X}_d = [X_1, X_2, \dots, X_{N_d}]^T \in \mathbb{C}^{N_d}$ is the original M -QAM data vector and the distorted frequency domain data symbol is given by $\tilde{\mathbf{X}}_d = \mathbf{X}_d + \mathbf{E}_d$, where $\mathbf{E}_d = [E_i]^T \in \mathbb{C}^{N_d}$, $i \in \Omega_d$. Since the decision regions for QAM are squares or half-squares, we allow square bounded (distortion) regions as well. We further divide a QAM constellation into internal points and external points. The external points can not only go inward in the bounded region but extend outward in the extended region. We require that the

frequency domain error vector \mathbf{E}_d satisfy the following constraints:

$$\begin{aligned}
& 1) \text{ if } Re(X_i) > \gamma : -\delta \leq Re(E_i) \leq \alpha\delta, \quad i \in \Omega_d \\
& 2) \text{ if } Re(X_i) < -\gamma : -\alpha\delta \leq Re(E_i) \leq \delta, \quad i \in \Omega_d \\
& 3) \text{ if } Im(X_i) > \gamma : -\delta \leq Im(E_i) \leq \alpha\delta, \quad i \in \Omega_d \\
& 4) \text{ if } Im(X_i) < -\gamma : -\alpha\delta \leq Im(E_i) \leq \delta, \quad i \in \Omega_d \\
& 5) \text{ if } -\gamma \leq Re(X_i) \leq \gamma : -\delta \leq Re(E_i) \leq \delta, \quad i \in \Omega_d \\
& 6) \text{ if } -\gamma \leq Im(X_i) \leq \gamma : -\delta \leq Im(E_i) \leq \delta, \quad i \in \Omega_d
\end{aligned} \tag{3.6}$$

and

$$\gamma = (\sqrt{M} - 2) \times \frac{d_{min}}{2}$$

where $M = 2^{2l}$, $l \in \mathbb{N}$, d_{min} is the minimum distance of the constellation, δ defines the allowable constellation error and $\alpha\delta$ decides the extended region. Note that γ is used to distinguish between internal and external points. Constraints 1)–4) are for external points while constraints 5)–6) are for internal points. We choose appropriate δ 's to satisfy different PAPR and BER requirements. Given $\delta = \epsilon$, our algorithm is designed to provide a modified OFDM constellation with the minimum achievable η .

In order to avoid increasing too much average transmit power, we set constraints on the TR pilots $\mathbf{E}_{TR} = [E_i]^T \in \mathbb{C}^{N_{TR}}$, where $i \in \Omega_{TR}$. We allow TR pilots to have exactly the same maximum power as that allowed in data subcarriers which carry signal points lie within the original constellation plus extended region. The TR constraints are thus given by

$$(\sigma + \alpha\delta) \leq Re(E_i) \leq \sigma + \alpha\delta, \quad i \in \Omega_{TR} \tag{3.7a}$$

$$(\sigma + \alpha\delta) \leq Im(E_i) \leq \sigma + \alpha\delta, \quad i \in \Omega_{TR} \tag{3.7b}$$

where $M = 2^{2l}, l \in \mathbb{N}$, and $\sigma = (\sqrt{M} - 1)d_{min}/2$ stands for the coordinate of external points.

Incorporating the above constraints, the proposed clipping scheme (inserted error vector) must satisfy the combined time and frequency domain constraints:

$$\tilde{\mathbf{x}} = \begin{cases} \|Re(\mathbf{x}) + Re(\mathbf{A}\hat{\mathbf{E}})\|_{\infty} \leq \eta \\ \|Im(\mathbf{x}) + Im(\mathbf{A}\hat{\mathbf{E}})\|_{\infty} \leq \eta \end{cases} \quad (3.8)$$

where

$$\mathbf{A} = \begin{pmatrix} \mathbf{Q}_C & -j\mathbf{Q}_S \\ j\mathbf{Q}_S & \mathbf{Q}_C \end{pmatrix} \quad \hat{\mathbf{E}} = \begin{pmatrix} Re(\mathbf{E}) \\ Im(\mathbf{E}) \end{pmatrix} \quad (3.9a)$$

are $(2NL \times 2N_t)$ and $2N_t \times 1$ matrices, respectively.

By introducing the $2N_t \times 1$ stacked vector $\hat{\mathbf{x}}$

$$\hat{\mathbf{x}} = \begin{pmatrix} Re(\mathbf{x}) \\ Im(\mathbf{x}) \end{pmatrix} \quad (3.10)$$

we restate the optimal clipper design problem as: Given \mathbf{X} , find the frequency domain error vector \mathbf{E} that satisfies the BD and TR constraints such that the resulting peaks η in both I- and Q-channels are minimized.

$$\begin{aligned} & \min \quad \eta \\ & \text{subject to : } \begin{pmatrix} \mathbf{A} & -\mathbf{1} \\ -\mathbf{A} & -\mathbf{1} \end{pmatrix} \begin{pmatrix} \hat{\mathbf{E}} \\ \eta \end{pmatrix} \preceq \begin{pmatrix} -\hat{\mathbf{x}} \\ -\hat{\mathbf{x}} \end{pmatrix} \end{aligned} \quad (3.11)$$

and

$$(a) \quad -\delta \leq Re(E_i) \leq \alpha\delta, \quad i \in \Omega_d, \quad \text{if } Re(X_i) > \gamma$$

$$(b) \quad -\alpha\delta \leq Re(E_i) \leq \delta, \quad i \in \Omega_d, \quad \text{if } Re(X_i) < -\gamma$$

$$(c) \quad -\delta \leq \text{Im}(E_i) \leq \alpha\delta, \quad i \in \Omega_d, \quad \text{if } \text{Im}(X_i) > \gamma$$

$$(d) \quad -\alpha\delta \leq \text{Im}(E_i) \leq \delta, \quad i \in \Omega_d, \quad \text{if } \text{Im}(X_i) < -\gamma$$

$$(e) \quad -\delta \leq \text{Re}(E_i) \leq \delta, \quad i \in \Omega_d, \quad \text{if } -\gamma \leq \text{Re}(X_i) \leq \gamma$$

$$(f) \quad -\delta \leq \text{Im}(E_i) \leq \delta, \quad i \in \Omega_d, \quad \text{if } -\gamma \leq \text{Im}(X_i) \leq \gamma$$

$$(g) \quad -(\sigma + \alpha\delta) \leq \text{Re}(E_i) \leq \sigma + \alpha\delta, \quad i \in \Omega_{TR}$$

$$(h) \quad -(\sigma + \alpha\delta) \leq \text{Im}(E_i) \leq \sigma + \alpha\delta, \quad i \in \Omega_{TR}$$

$$\text{in variables: } \hat{\mathbf{E}} \in \mathbb{R}^{2N_t}, \quad \hat{\mathbf{x}} \in \mathbb{R}^{2NL}$$

where $\mathbf{1}$ denotes a $2NL \times 1$ vectors, and η is real-valued. Note that (a) \sim (f) are the BD constraints while (g) \sim (h) are the TR constraints.

3.4 Simulation Results

In this section, we provide some numerical performance of our algorithm and an example of time- and frequency-domain signal of original and optimized signal. We consider an OFDM system with 256 subcarriers using 16-QAM modulation for the data carried on each available subcarrier. Only 128 tones are used to carry data, and there are six reserved tones at subcarriers 193, 194, 195, 196, 197, 198, respectively. 0 denotes dc tone and guard-bands are distributed in subcarriers 0 to 64 and 199 to 256. The reserved tones' locations do not affect the PAPR value too much but the number of the reserved tones does. The more tones are reserved, the higher the PAPR reduction gain becomes. For fair comparison, the number of reserved tones is the same for all schemes whose performance is presented in this section.

To begin with, we examine the clipping effects in time and frequency domains. Fig. 3.5. shows the original time-domain signal of an OFDM symbol with a PAPR of 9.6448 dB. After applying the proposed nonlinear clipping algorithm (3.11), the resulting time-domain signal is plotted in Fig. 3.6 where the PAPR is reduced to 5.9015

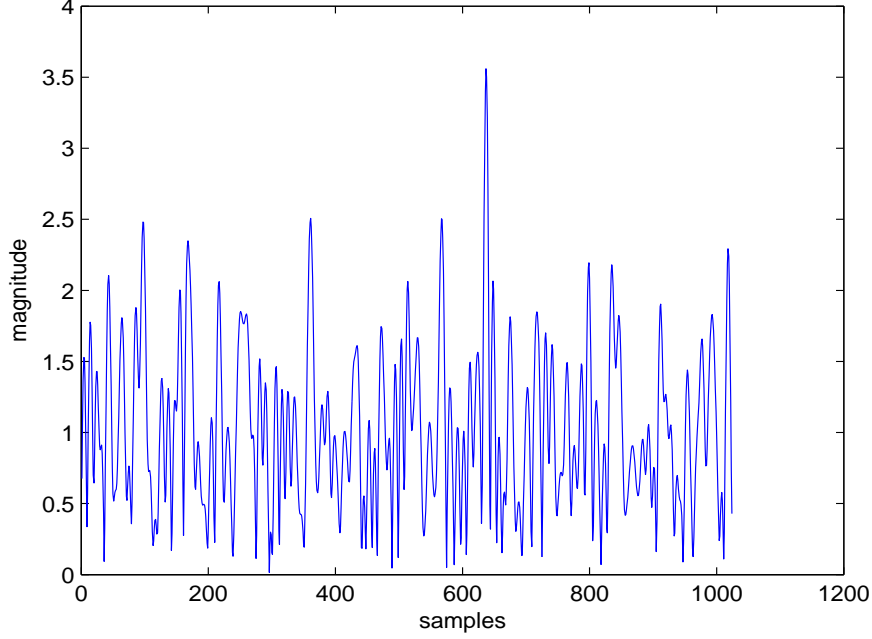


Figure 3.5: Original time-domain signal with PAPR=9.6448 dB.

dB. However, we achieve such PAPR reduction at the cost of a smaller minimum distance in the 16-QAM constellation. The constellation setup for our case is 16-QAM having $\{-\frac{3d_{min}}{2}, -\frac{d_{min}}{2}, \frac{d_{min}}{2}, \frac{3d_{min}}{2}\}$ as signal points on real and imaginary axes (I- and Q-channel components) with a maximum constellation error $\delta = 0.05d_{min}$. Red stars in Fig. 3.7 are clipped frequency domain samples which has deviated from the original constellation points and the resulting minimum distance for this case is reduced to $0.9d_{min}$. A shorter minimum distance means worse BER performance, but larger distortion bound and extended region give better PAPR reduction capability. There is an obvious tradeoff between the PAPR reduction and BER performance degradation.

Fig. 3.8 shows the phase difference (original phase - optimized phase) and amplitude trajectories of a typical time-domain sequence before and after performing the proposed nonlinear clipping. Obviously, our clipping method does result in (or allow) phase rotations of the time domain samples. Separate constraints on I- and Q-channel magnitudes result in envelop clipping and phase rotation (in this example as much as 0.2180 ra-

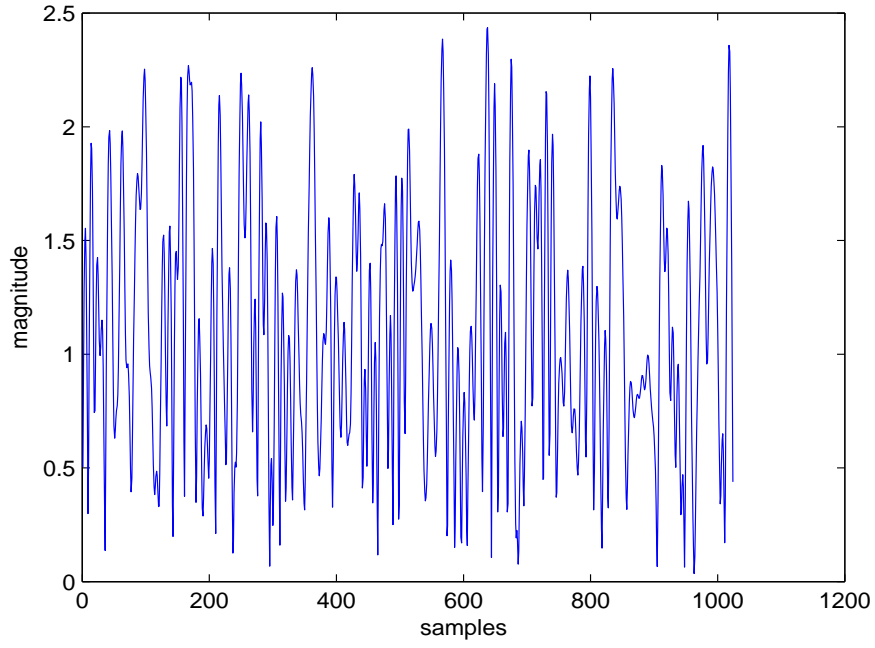


Figure 3.6: Clipped time-domain signal with PAPR=5.9015 dB.

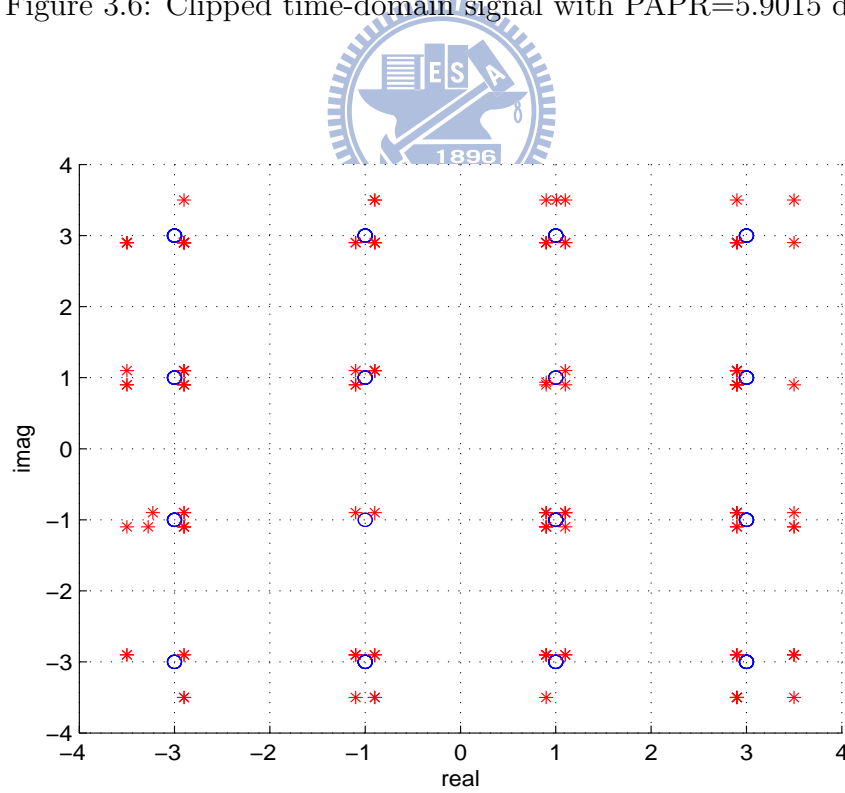


Figure 3.7: Constellation of distorted frequency-domain signal achieving 3.7433 dB PAPR reduction.

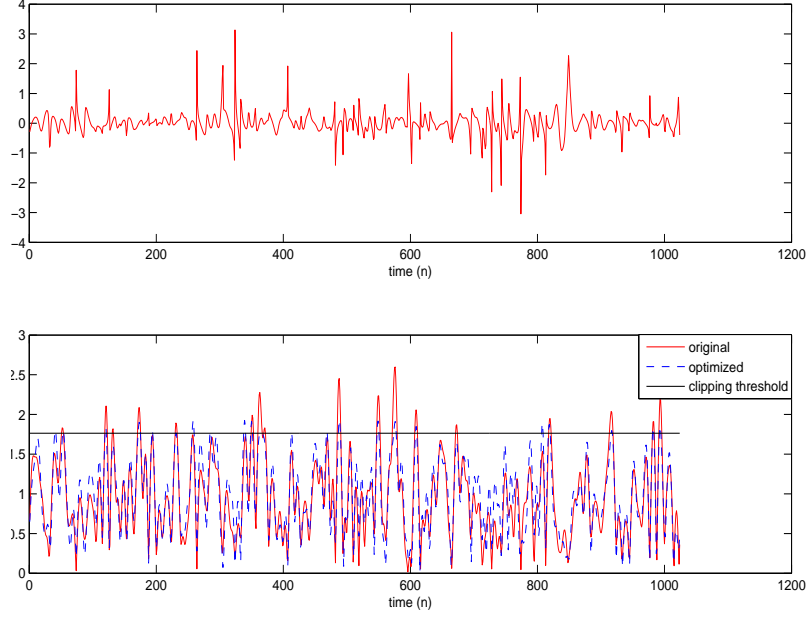


Figure 3.8: Phase difference and amplitude trajectories of a typical time-domain sequence before and after nonlinear clipping.

dian). As mentioned before, phase rotation gives us an extra degree of freedom for PAPR reduction. The optimal rotated phase is obtained by solving the corresponding CLP problem (3.11).

Simulated BER performance of the conventional OFDM and error vector optimized OFDM schemes in AWGN channels is given in Fig. 3.10. As expected, the larger the allowed constellation error is, the greater the PAPR reduction becomes. As mentioned before, since the constellation (frequency domain) error reduces the minimum-distance of the signal set, it also degrades the BER performance. In this figure we find that a constellation error bound of $\delta = 0.05d_{min}$ gives BER performance better than that with a bounded error of $\delta = 0.1d_{min}$. It is clear that the amount of PAPR reduction is an increasing function of the allowed frequency domain distortion bound.

Figs. 4.6. and 3.10 indicate that our clipping scheme yields a better PAPR performance than that achieved by RCF-BD while maintaining the same BER performance. This PAPR reducing gain is due to the fact that the error vector used in RCF-BD has

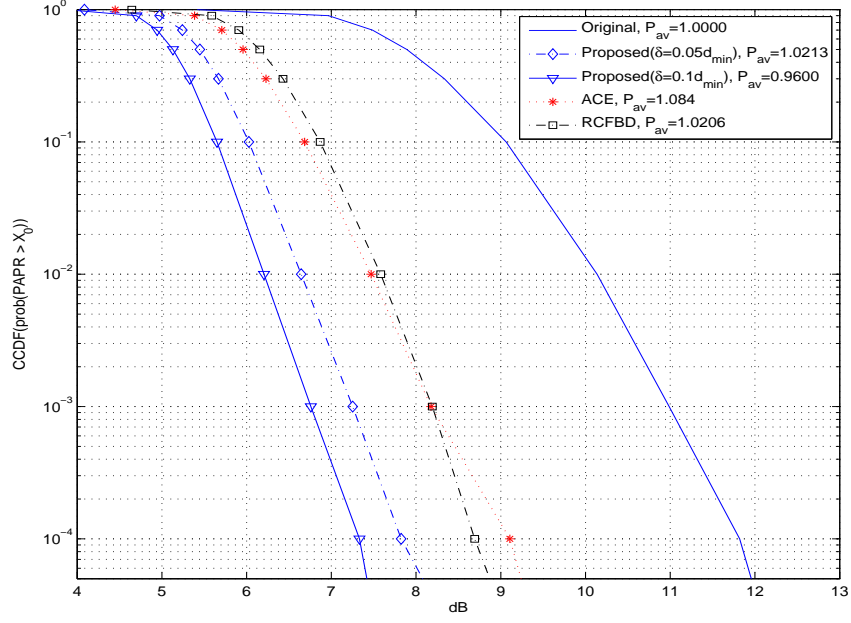


Figure 3.9: Effective PAPR gain for 16-QAM 256-carrier OFDM symbol with $L=4$ over-sampling for $\delta = 0.05d_{min}$, $\delta = 0.1d_{min}$, ACE, RCFBD, and separated coordinate PAPR.

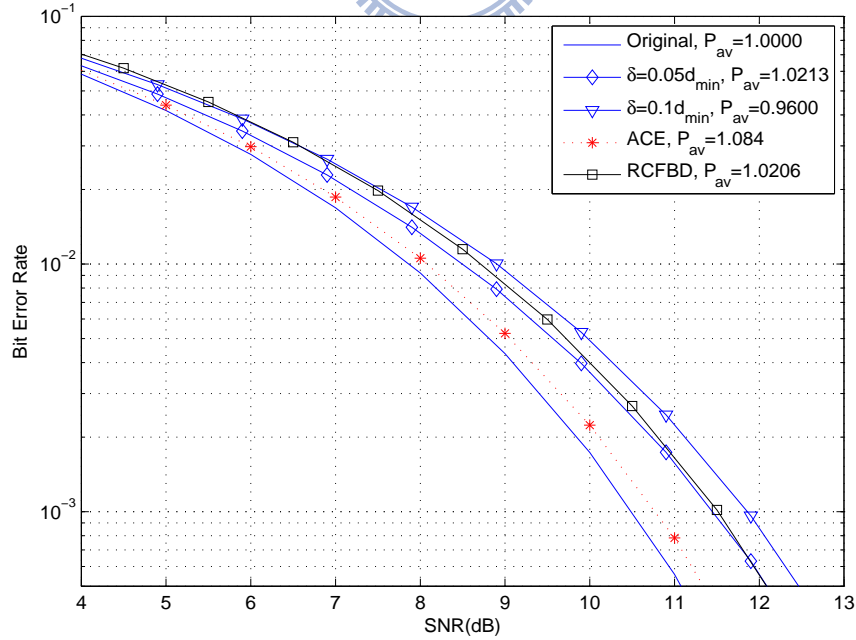


Figure 3.10: BER of a 16-QAM and 256-carrier OFDM system.

not been optimized.

Although both ours and the ACE schemes use an optimization procedure to reduce PAPR, and our algorithm outperforms the ACE scheme by imposing BD's. A BD region allows optimal modifications for distorted data points, it enlarges the feasible set of linear programming problem whence leads to a greater likelihood to find a solution with lower PAPR.

3.5 Chapter Summary

In this chapter we present a novel nonlinear clipping technique that extends the RCF-BD and TR concepts to reduce the PAPR of OFDM signals. We formulate the proposed algorithm as one for solving a CLP problem. The solution can be easily found by following the established procedure. The proposed approach does not have to modify the receiver structure and needs not to send side information. Moreover, our algorithm guarantees that the optimal error vector is obtained and the resulting PAPR value is minimized under certain BD constraints. The complexity of our algorithm can be greatly reduced by if a fast algorithm to solve the corresponding CLP problem can be found.

Chapter 4

Selective Mapping without Side Information

4.1 Background

The basic idea of selective mapping (SLM) is to scramble an OFDM frame (symbol) by a set of known sequences of the same length and select the scrambled (SLM-encoded) one with the smallest PAPR for transmission.

For uncorrelated SLM sequences, the resulting SLM-encoded OFDM signals and the corresponding PAPR's will be uncorrelated. Hence if the PAPR ratio for original OFDM symbol has probability p of exceeding a certain level, the probability for the OFDM symbol using k SLM sequences is decreased to p^k .

There are three major design issues related to the SLM scheme, namely, encoder and decoder complexities, SLM sequences design, and side information (SI) about the scrambling sequence. The designs presented in this chapter emphasize the latter two concerns while the complexity is considered as a secondary issue. We proposed a sequence design which hides SI in each SLM sequence. Since each sequence is distinguishable, a blind sequence detector can be used at receiver and data throughput is increased. In addition, the implementation of proposed sequences are easy and memory usage is less.

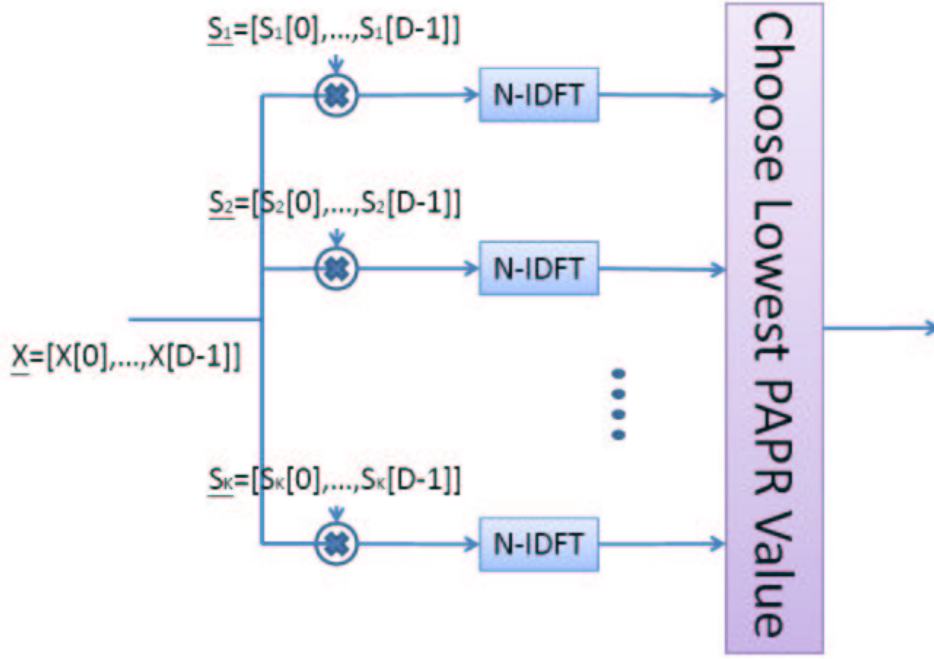


Figure 4.1: Original SLM encoder.

4.2 System Model

Consider an OFDM system which transmits frequency domain OFDM symbol $\mathbf{x} = [x(0), x(1), \dots, x(N-1)]$ in parallel using N sub-carriers f_l , $l = 0, 1, 2, \dots, N-1$ with frequency spacing $\Delta f = \frac{1}{T}$, T being the symbol duration without the cyclic prefix (CP). We assume that $x(i) \in \mathbb{Q}$ are M -PSK symbols whence \mathbb{Q} is the set of constellation points. To reduce the resulting PAPR, \mathbf{x} is modified by one of sequences in the set $\{\mathbf{s}_k = [s_0^k, s_1^k, \dots, s_{N-1}^k] : k \in \mathbb{K}\}$, where k is the sequence index and \mathbb{K} can be regarded as the set of selective mapping sequences.

The SLM encoder chooses the encoded sequence \mathbf{y} which resulting in a modified sequence with the smallest PAPR value. In other words, neglecting the cyclic prefix, the transmitted frequency domain sequence is given by

$$\mathbf{y} = \mathbf{s}_i \odot \mathbf{x}, \quad i = \arg \min_{k \in \mathbb{K}} \text{PAPR}\{\text{IDFT}(\mathbf{s}_k \odot \mathbf{x})\} \quad (4.1)$$

where \odot represents the Hadamard product.

After removing the prefix part and assuming perfect receiver synchronization, the received signal can be expressed as

$$\mathbf{r} = \mathbf{h} \odot \mathbf{y} + \mathbf{w} = \mathbf{h} \odot \mathbf{s}_i \odot \mathbf{x} + \mathbf{w} \quad (4.2)$$

where $\mathbf{h} = [h_0, h_1, \dots, h_{N-1}]$ is the frequency-domain channel response (CR) and \mathbf{w} is an zero mean white Gaussian noise vector with covariance $\sigma_n^2 \mathbf{I}$. Since the operation \odot is commutative and $\mathbf{s}_i^* \odot \mathbf{r} = \mathbf{h} \odot \mathbf{x} + \mathbf{w}'$, where \mathbf{w}' has the same statistical distribution as \mathbf{w} , if \mathbf{h} and the mapping sequence \mathbf{s}_k are known, then

$$\mathbf{s}_k^* \odot \mathbf{h}^* \odot \mathbf{r} \odot |\mathbf{h}|^{-2} = \mathbf{x} + \mathbf{v} \stackrel{def}{=} \mathbf{r}' \quad (4.3)$$

where $|\mathbf{h}|^{-2} = [|h_0|^{-2}, |h_1|^{-2}, \dots, |h_{N-1}|^{-2}]$ and $\mathbf{v} = [v_0, v_1, \dots, v_{N-1}]$ is a vector of independent (but not identically) distributed Gaussian random variables. Under this circumstance, the ML data detector is given by

$$\hat{\mathbf{x}}(\mathbf{s}_k, \mathbf{h}) \stackrel{def}{=} \hat{\mathbf{x}}_k = D[\mathbf{r}'] \quad (4.4)$$

where $D[\mathbf{r}']$ is the vector obtained by making componentwise MPSK decisions.

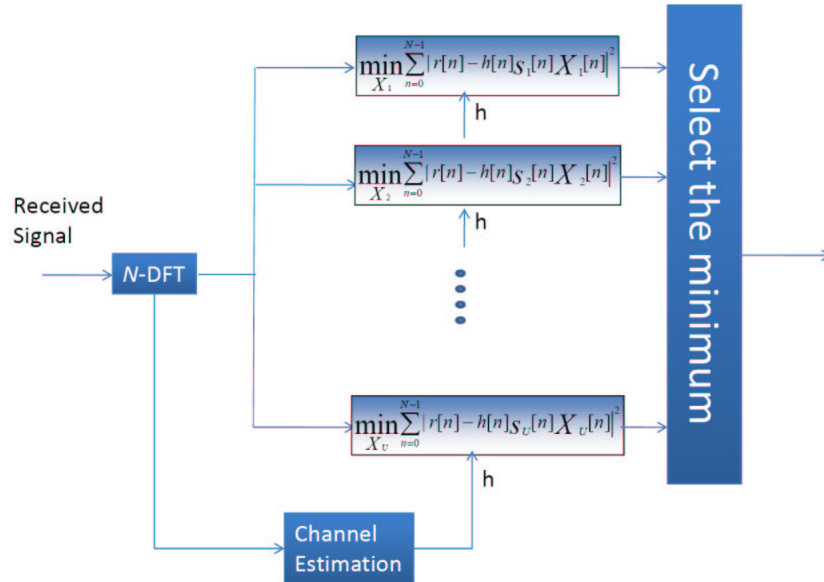


Figure 4.2: SLM decoder proposed by Tellambura and Jayalath in [10].

The above discussion suggests that, when the true CR is known, the optimal detector is

$$(\hat{\mathbf{x}}, \hat{\mathbf{s}}) = \arg \min_{k \in \mathbb{K}} L(\mathbf{r}, \hat{\mathbf{x}}_k; \mathbf{s}_k) \quad (4.5)$$

where

$$L(\mathbf{r}, \hat{\mathbf{x}}_k; \mathbf{s}_k) = \sum_{n=0}^{N-1} ||r[n] - h[n]s_k[n]\hat{x}_k[n]||^2 \quad (4.6)$$

The pairwise error probability (PEP) $P[(\hat{\mathbf{x}}_i, \mathbf{s}_i) \rightarrow (\hat{\mathbf{x}}_k, \mathbf{s}_k) | \mathbf{h}]$ that the transmitted 2-tuple $(\hat{\mathbf{x}}_i; \mathbf{s}_i)$ is erroneously decoded as $(\mathbf{x}_k, \hat{\mathbf{s}}_k)$ is given by

$$P[(\hat{\mathbf{x}}_i, \mathbf{s}_i) \rightarrow (\hat{\mathbf{x}}_k, \mathbf{s}_k) | \mathbf{h}] = P\{L(\mathbf{r}, \hat{\mathbf{x}}_k, \mathbf{s}_k) \geq L(\mathbf{r}, \hat{\mathbf{x}}_i, \mathbf{s}_i)\} \quad (4.7)$$

Since

$$L(\mathbf{r}, \hat{\mathbf{x}}_k; \mathbf{s}_k) \geq L(\mathbf{r}, \hat{\mathbf{x}}_i; \mathbf{s}_i) \quad (4.8)$$

or equivalently,

$$\sum_{n=0}^{N-1} ||r[n] - h[n]s_k[n]\hat{x}_k[n]||^2 \geq \sum_{n=0}^{N-1} ||r[n] - h[n]s_i[n]\hat{x}_i[n]||^2 \quad (4.9)$$

the PEP can be calculated as

$$\begin{aligned} & P[(\hat{\mathbf{x}}_i, \mathbf{s}_i) \rightarrow (\hat{\mathbf{x}}_k, \mathbf{s}_k) | \mathbf{h}] \\ &= \prod_{n=0}^{N-1} Q\left(\sqrt{\frac{2 ||h[n]||^2 ||s_i[n]\hat{x}_i[n] - s_k[n]\hat{x}_k[n]||^2}{N_o}}\right) \end{aligned} \quad (4.10)$$

Using the Chernoff bound

$$Q(x) \leq \exp(-x^2/2) \quad (4.11)$$

we obtain

$$\begin{aligned} & P[(\hat{\mathbf{x}}_i, \mathbf{s}_i) \rightarrow (\hat{\mathbf{x}}_k, \mathbf{s}_k) | \mathbf{h}] \\ &\leq \prod_{n=0}^{N-1} \exp(-||h[n]||^2 ||s_i[n]\hat{x}_i[n] - s_k[n]\hat{x}_k[n]||^2) \\ &= \exp\left(-\sum_{n=0}^{N-1} ||h[n]||^2 ||s_i[n]\hat{x}_i[n] - s_k[n]\hat{x}_k[n]||^2\right) \end{aligned} \quad (4.12)$$

For AWGN or slow fading channels, the upper-bound becomes

$$P[(\hat{\mathbf{x}}_i, \mathbf{s}_i) \rightarrow (\hat{\mathbf{x}}_k, \mathbf{s}_k)|h_o] \leq \exp(-h_w^2 \|\mathbf{s}_i \hat{\mathbf{x}}_i - \mathbf{s}_k \hat{\mathbf{x}}_k\|_2^2) \quad (4.13)$$

where $h_w = 1/N_0$ (AWGN) or $h_w = \min_n h[n]$ (slow fading). Assuming equally signaling and defining

$$D_i = \min_{k \neq i, k \in \mathbb{K}} \|\mathbf{s}_i \odot \hat{\mathbf{x}}_i - \mathbf{s}_k \odot \hat{\mathbf{x}}_k\|_2^2 \quad (4.14)$$

we express the average conditional symbol error probability (SEP) as

$$\begin{aligned} P_s(e) &\leq \sum_{i \in \mathbb{K}} \sum_{k \in \mathbb{K} - \{i\}} P(\mathbf{s}_i) P[(\hat{\mathbf{x}}_i, \mathbf{s}_i) \rightarrow (\hat{\mathbf{x}}_k, \mathbf{s}_k)|h_o] \\ &\leq \frac{1}{|\mathbb{K}|} \sum_{i \in \mathbb{K}} \exp(-h^2 D_i) \end{aligned} \quad (4.15)$$

To minimize the average SEP, the minimum Euclidean distance between \mathbf{s}_i and any other sequences, D_i , should be maximized and which leads to an optimization problem that could be formulated as follow:

$$\begin{aligned} \max \quad & D_i \\ \text{s.t.} \quad & \mathbf{s}_i = [e^{j\phi_0^i}, e^{j\phi_1^i}, \dots, e^{j\phi_{N-1}^i}], \phi_n^i \in [0, 2\pi) \\ & \mathbf{s}_k = [e^{j\phi_0^k}, e^{j\phi_1^k}, \dots, e^{j\phi_{N-1}^k}], \phi_n^k \in [0, 2\pi) \\ & i \in \mathbb{K}, k \in \mathbb{K} - \{i\} \end{aligned}$$

$$\text{where } D_i = \min_{i \neq k, i, k \in \mathbb{K}} \|\mathbf{s}_i \odot \hat{\mathbf{x}}_i - \mathbf{s}_k \odot \hat{\mathbf{x}}_k\|_2^2 \quad (4.16)$$

For frequency selective fading channels with subcarrier spacing greater than the coherent bandwidth, $h[n]$'s can be modelled as identical and independent distributed random variables, hence we have [10]

$$\begin{aligned} &P[(\mathbf{s}_i, \hat{\mathbf{x}}_i) \rightarrow (\mathbf{s}_k, \hat{\mathbf{x}}_k)|\mathbf{h}] \\ &\simeq \frac{(2^{N-1}/N)(\text{SNR})^{-2N}}{\prod_{n=0}^{N-1} |s_i[n]\hat{x}_i[n] - s_k[n]\hat{x}_k[n]|^2} \end{aligned} \quad (4.17)$$

where $\prod_{n=0}^{N-1} |s_i[n]\hat{x}_i[n] - s_k[n]\hat{x}_k[n]|^2$ is the product distance between $(\mathbf{s}_i, \hat{\mathbf{x}}_i)$ and $(\mathbf{s}_k, \hat{\mathbf{x}}_k)$.

4.3 Sequence design criteria

When M -PSK modulation is applied, the expected value of relative Euclidean distance between arbitrary two length- N SLM sequences of SLM decoder proposed in [10] can be calculated as

$$\begin{aligned} D_{lb} &= \frac{NM}{\pi} 2 \int_0^{\frac{\pi}{M}} \sin \frac{\theta}{2} d\theta \\ &= \frac{4MN}{\pi} (1 - \cos \frac{\pi}{2M}) \end{aligned} \quad (4.18)$$

It can be proved that any polyphase sequences can have larger expected minimum pairwise distance than D_{lb} .

By observing this fact, two criteria have be found:

- 1) Every entry of a sequence should have distinct value to corresponding entry of any other sequence. That means a nonzero minimum distance shall be preserved between the corresponding entry of arbitrary two sequences.
- 2) The magnitude of entries of SLM sequences is constant magnitude 1. Variable magnitude might cause noise enhancement at receiver site.

To accomplish the above two criteria, unit circle shall be discretized into finite and equal-spaced points, and every entry of sequences has to take a value among all these discrete points. In addition, the discretizing process ensures sequences become polyphase, thus generalized Euclidean distance D_i is larger than D_{lb} . After the discretizing process, the discrete total distance space is limited. Our goal is to minimize the blind detection error rate, thus one more design criterion is introduced:

- 3) Because of the lack of prior knowledge of sequence selection, each sequence has the same probability of being selected. By observing equation (4.15), A obvious solution is to have all the pairwise distance to be equal. Therefore, D_i should be forced to be equal to D_{avg} for all i .

where D_{avg} will be provided in section V. we introduce group theory and use prime number finite field to construct a set of sequences which could have equal pairwise distance. Proposed sequence design is optimal in the sense of discrete phase and is easily constructed, in the mean time, memory requirement is less.

For the next two sections, we will first review the structure of the cyclic group G and the definition of characters of finite field $GF(p)$, and then use the knowledge of group theory to construct a set of sequences which satisfies these three criteria.

4.4 A Review on Group Theory

Let a be a generator of the finite cyclic group G , i.e., $G = \langle a \rangle = \{a^n, n \in \mathbb{Z}\}$, \mathbb{Z} being the set of integers, and denote the order of a by $o(a)$, the cardinality of G by $|G|$. We immediately have $|G| = |\langle a \rangle| = o(a)$. Furthermore, if $|G| = p$ is prime then any non-identity element of G is a generator, i.e., $G = \langle g \rangle$ and $o(g) = p, \forall g \in G \setminus \{e\}$, where e is the identity of G .

The set of all p th roots of unity in G , $U_p(G) = \{a | o(a) = p, a \in G\}$ is obviously a cyclic group under the multiplication operation as $\forall a, b \in U_p(G), (ab)^p = a^p b^p = e \Rightarrow ab \in U_p(G)$. Now if G is the set of complex numbers, \mathbb{C} , then $e = 1$ and $U_p(\mathbb{C}) = \{e^{j2\pi k/p}, k = 1, 2, \dots, p\}$. By denoting $W_p = e^{j2\pi/p}$, we have $U_p(\mathbb{C}) = \langle W_p^k \rangle$, for all k . An alternative statement is

Property 1. Define the listing vector generated by the seed g , where g is a p th root of unit, then $\mathbf{s}(g) = (g^0, g^1, \dots, g^{(p-1)})$. Two listing vectors generated by different seeds are permuted version of each other, i.e.,

$$\mathbf{s}(W_p^m) = \mathbf{s}(W_p^n) \mathbf{P}, \forall m \neq n \in \mathbb{Z} \setminus \{0\} \quad (4.19)$$

where \mathbf{P} is a permutation matrix.

Note that $\mathbf{s}(W_p^0) = (1, 1, \dots, 1)$ is the all-1 vector.

4.5 Proposed SLM Sequence Design

In this section, we will apply our knowledge of group characters to present proposed sequence design for general M -PSK modulation and give an example of SLM sequences under QPSK modulation.

Since (4.14) is the combination of \mathbf{s} and M -PSK data $\mathbf{x}, \hat{\mathbf{x}}$. Data effect shall be taken into consideration. the ML decoder only count the relative distance from de-SLM symbol to the nearest constellation point, every decision region is equivalent in the sense of calculating relative distance. For M -PSK, there are M decision boundaries and every division is equivalent. The proposed sequences design consists of two parts, the deterministic part \mathbf{s}_d and the data scrambling part \mathbf{s}_r . The SLM sequences are obtained by element-wise multiplying these two parts.

$$\mathbf{s} = \mathbf{s}_d \odot \mathbf{s}_r \quad (4.20)$$

The deterministic part is to have entries of sequences in one decision boundary to have distinguishable value in the relative distance fashion. Second, the data scrambling part is to randomly chooses one among all equivalent divisions to make encoded vector uncorrelated. Since prime p cyclic group $S(p)$ is chosen for SLM sequences, each subgroup of this cyclic group forms the deterministic part. And the primitive element of $S(p)$ is W_{Mp}^1 , Mp -th root of unity.

The expression of sequence generated by element g_k is

$$\begin{aligned} \mathbf{S}(g_k) &= [\mathbf{s}(g_k^1), \mathbf{s}(g_k^2), \dots, \mathbf{s}(g_k^{(p-1)})] \\ &= [W_{Mp}^k, W_{Mp}^{2k}, \dots, W_{Mp}^{(p-1)k}] \end{aligned} \quad (4.21)$$

is an $M \times p$ matrix. Each column of $\mathbf{S}(g_k)$ is constructed by $\mathbf{s}(g_k^n)$.

Lemma 1. : *The pairwise distance between arbitrary two sequences which are constructed by different generated elements are equal. $D(\mathbf{S}(g_{k_1}), \mathbf{S}(g_{k_2})) = D(\mathbf{S}(g_{k_1}), \mathbf{S}(g_{k_3}))$, $g_{k_1}, g_{k_2}, g_{k_3} \in GF(p)$.*

Proof: *Lemma 1* can be easily shown by *Preliminary 2* that each sequence has permutation relation to any other sequence. And the detail proof can be referred to *Appendix*. And the subtraction of arbitrary two sequences also has permutation relation. Therefore, the pairwise distance is equal for arbitrary two sequences. If distance of a complete distance is defined as d , then the minimum pairwise distance of arbitrary two sequences is

$$D(\mathbf{S}(g_{k_1}), \mathbf{S}(g_{k_2})) = d \quad (4.22)$$

By *Lemma 1*, we can satisfy the third design criterion that pairwise distance of arbitrary two sequences is equal.

Lemma 2. : *The pairwise distance of any two sequences is equal to D_{avg} .*

Proof Entries of all sequences with same index are a complete period of finite field, such that the total distance space for length- $p - 1$ sequences within a decision region is $(p - 1)d$, and the average distance is $D_{avg} = d$. It is easy to see that D_{avg} is equal to (4.22).

It is believed that the randomness in frequency domain is inversely proportional to the PAPR value of the OFDM symbol. Our goal is to have uncorrelated SLM sequences. Hence, the data scrambling part of proposed SLM sequences has to be uncorrelated, so $\mathbf{s}_r^k = [s_r^k[1], s_r^k[2], \dots, s_r^k[p - 1]]$, the data scrambling part of k -th sequence is generated by probability mass function (pmf)

$$P(r_n = s) = \frac{1}{M}, \quad s = 1, 2, \dots, M, \quad n = 0, \dots, p - 1 \quad (4.23)$$

and each entry $s_r^k[n]$ is to indicate which division is used. s_r^k is corresponding to the location of 1 in the row of the matrix \mathbf{U}_k and others are zeros, and we can have a indicator vector by multiplying \mathbf{U}_k with division matrix $\mathbf{D} = [e^{\frac{j2\pi}{M}}, \dots, e^{\frac{j2\pi(M-1)}{M}}]^T$ which consists of representations of all decision boundaries of M-PSK. Then the data scrambling \mathbf{s}_r part of sequence can be represented as

$$\mathbf{s}_r^k = (\mathbf{U}_k \mathbf{D})^T \quad (4.24)$$

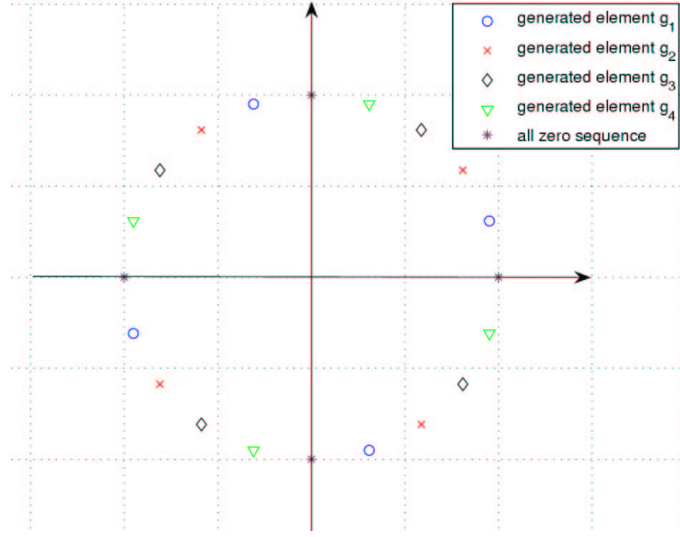


Figure 4.3: Distribution of generated element g_k on unit circle.

In the following, we provide an example of $p = 5$, QPSK SLM sequences. In QPSK modulation, the primitive element is $W_{4 \times 5}^1 = W_{20}^1$ and the data effect phase vector $\mathbf{D} = [W_4^0, W_4^1, W_4^2, W_4^3]^T$ and the SLM sequence with generator element g_1 is

$$\mathbf{S}(g_1) = [W_{20}^{1 \times 1}, W_{20}^{2 \times 1}, W_{20}^{3 \times 1}, W_{20}^{4 \times 1}]$$

The sequences with generator elements g_2 , g_3 , and g_4 are

$$\mathbf{S}(g_2) = [W_{20}^{1 \times 2}, W_{20}^{2 \times 2}, W_{20}^{3 \times 2}, W_{20}^{4 \times 2}]$$

$$\mathbf{S}(g_3) = [W_{20}^{1 \times 3}, W_{20}^{2 \times 3}, W_{20}^{3 \times 3}, W_{20}^{4 \times 3}]$$

$$\mathbf{S}(g_4) = [W_{20}^{1 \times 4}, W_{20}^{2 \times 4}, W_{20}^{3 \times 4}, W_{20}^{4 \times 4}]$$

Then we have to choose one combination out of all possible sequences, we use matrix \mathbf{U}_k , $k \in \mathbb{K}$ to determine which expression is taken.

Ex. $\mathbf{u}_1 = [1, 3, 2, 2]$ implies that matrix \mathbf{U}_1 is

$$U_1 = \begin{pmatrix} 1 & 0 & 0 & 0 \\ 0 & 0 & 1 & 0 \\ 0 & 1 & 0 & 0 \\ 0 & 1 & 0 & 0 \end{pmatrix}$$

and the corresponding sequence with generator element g_1 is

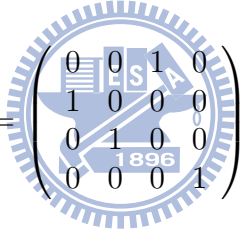
$$\begin{aligned}\mathbf{s}_1 &= [W_{20}^{1 \times 1}, W_{20}^{2 \times 1}, W_{20}^{3 \times 1}, W_{20}^{4 \times 1}] \odot (\mathbf{U}_1 \mathbb{D})^T \\ &= [W_{20}^{1 \times 1}, W_{20}^{2 \times 1} W_4^2, W_{20}^{3 \times 1} W_4^1, W_{20}^{4 \times 1} W_4^1]\end{aligned}$$

Sequence with generator element g_2 with random vector $\mathbf{u}_2 = [1, 1, 4, 2]$ and the matrix \mathbf{U}_2 is

$$\mathbf{U}_2 = \begin{pmatrix} 1 & 0 & 0 & 0 \\ 1 & 0 & 0 & 0 \\ 0 & 0 & 0 & 1 \\ 0 & 1 & 0 & 0 \end{pmatrix}$$

$$\begin{aligned}\mathbf{s}_2 &= [W_{20}^{1 \times 2}, W_{20}^{2 \times 2}, W_{20}^{3 \times 2}, W_{20}^{4 \times 2}] \odot (\mathbf{U}_2 \mathbb{D})^T \\ &= [W_{20}^{1 \times 2}, W_{20}^{2 \times 2}, W_{20}^{3 \times 2} W_4^3, W_{20}^{4 \times 2} W_4^1]\end{aligned}$$

Sequence with generator element g_3 with random vector $\mathbf{u}_3 = [3, 1, 2, 4]$ and the matrix \mathbf{U}_3 is



$$\mathbf{U}_3 = \begin{pmatrix} 0 & 0 & 1 & 0 \\ 1 & 0 & 0 & 0 \\ 0 & 1 & 0 & 0 \\ 0 & 0 & 0 & 1 \end{pmatrix}$$

$$\begin{aligned}\mathbf{s}_3 &= [W_{20}^{1 \times 3}, W_{20}^{2 \times 3}, W_{20}^{3 \times 3}, W_{20}^{4 \times 3}] \odot (\mathbf{U}_3 \mathbb{D})^T \\ &= [W_{20}^{1 \times 3} W_4^3, W_{20}^{2 \times 3}, W_{20}^{3 \times 3} W_4^1, W_{20}^{4 \times 3} W_4^3]\end{aligned}$$

Sequence with generator element g_4 with random vector $\mathbf{u}_4 = [2, 4, 1, 1]$ and the matrix \mathbf{U}_4 is

$$\mathbf{U}_4 = \begin{pmatrix} 0 & 1 & 0 & 0 \\ 0 & 0 & 0 & 1 \\ 1 & 0 & 0 & 0 \\ 1 & 0 & 0 & 0 \end{pmatrix}$$

$$\begin{aligned}\mathbf{s}_4 &= [W_{20}^{1 \times 4}, W_{20}^{2 \times 4}, W_{20}^{3 \times 4}, W_{20}^{4 \times 4}] \odot (\mathbf{U}_4 \mathbb{D})^T \\ &= [W_{20}^{1 \times 4} W_4^1, W_{20}^{2 \times 4} W_4^3, W_{20}^{3 \times 4}, W_{20}^{4 \times 4}]\end{aligned}$$

Once we generate \mathbf{u}_k , $k = 1, \dots, p-1$ from uniform distribution in (4.23), it is fixed and should be known for both transmitter and receiver side.

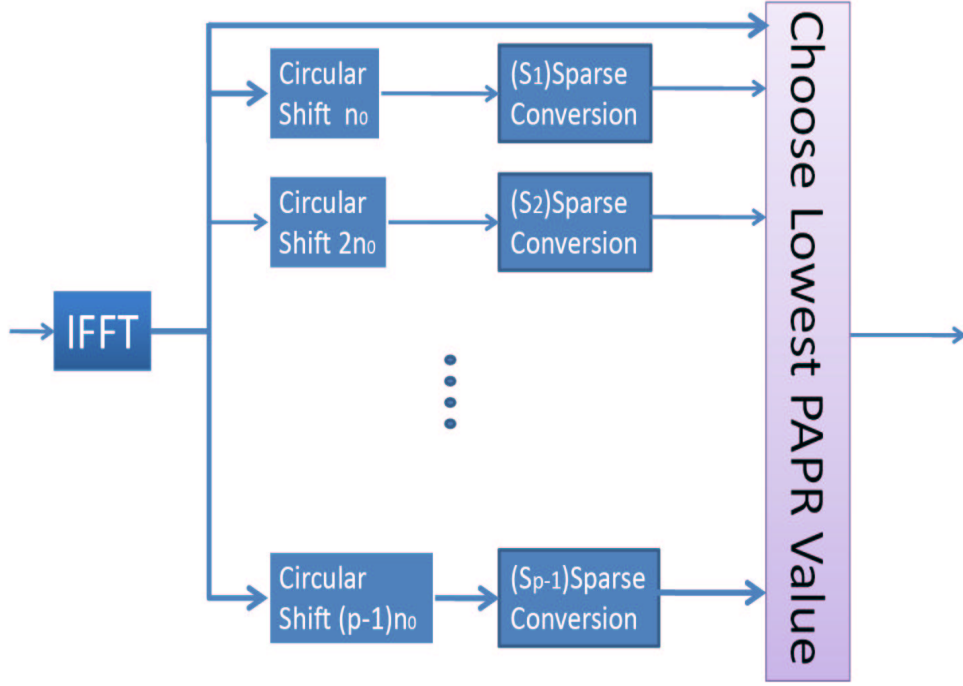


Figure 4.4: Block diagram of low complexity SLM encoder.

4.6 Low Complexity SLM Encoder

An SLM scheme using U SLM sequences needs U IFFT operations to complete the encoding. Since proposed SLM sequences have good properties that sequences are combined with deterministic term and data scrambling term, the encoding procedure of SLM using proposed SLM sequences can be simplified by using several circular shift units and conversion blocks.

For the modified encoder, the deterministic part of our SLM sequence generated by $g_k, k = 1, \dots, p - 1$ is

$$\begin{aligned} \mathbf{S}(g_k) &= [\mathbf{s}(g_k^1), \mathbf{s}(g_k^2), \dots, \mathbf{s}(g_k^{(p)})] \\ &= [W_{Mp}^k, W_{Mp}^{2k}, \dots, W_{Mp}^{(p)k}] \end{aligned} \quad (4.25)$$

which is obtained by using an $k \times n_0 = k \times \frac{NL}{Mp}$ circular shift in time domain where N is number of sub-channel, L is over-sampling factor, M denotes M -PSK, and p is chosen for prime group.

A time-frequency fourier transform pair has a up/down sampling property that if frequency domain sequence is repeated l times, time domain pair is up-sampled l times.

Ex. $[a, b, c, d]$ - $[e, f, g, h]$ is a frequency-time fourier pair where $[a, b, c, d]$ is frequency domain sequence and $[e, f, g, h]$ is time domain pair of $[a, b, c, d]$. If $[a, b, c, d]$ is repeated 2 times and becomes $[a, b, c, d, a, b, c, d]$, time domain pair becomes $[e, 0, f, 0, g, 0, h, 0]$.

We would take this property to implement the data scrambling part of proposed SLM sequences. First, $(p - 1)$ 4-tuple sequences are randomly selected from scrambling set $\{1, j, -1, -j\}$ which has 256 combinations in total. Each chosen sequence is repeated $\frac{N}{4}$ times and becomes a length N sequence, and in effect the corresponding time domain vector \mathbf{t}_u will be N -tuple sequence with only 4 non-zero entries. A sparse conversion matrix \mathbf{S}_u can be formed as

$$\mathbf{S}_u = [\mathbf{t}_u^{(0)}, \mathbf{t}_u^{(1)}, \dots, \mathbf{t}_u^{(NL-1)}] \quad (4.26)$$

where $\mathbf{t}_u^{(k)}$ is the circularly down-shifted version of the column vector $\mathbf{t}_u^{(0)}$ by k elements. And sparse matrix operation has less complexity than IFFT and circular convolution.

Frequency domain operation of proposed SLM sequences can be seen as circular shift in time domain followed by circular convolution with a sparse signal. Deterministic part is a circular shift operation of data vector and scrambling part can be done by convolution with a sparse signal. Hence, the encoding procedure is shown in fig. 4.4 that frequency data vector is converted to time domain vector once. Then each branch represents a circular shift and a sparse conversion for corresponding SLM sequence.

Since the proposed low complexity SLM encoder needs cyclic shift by $k \times n_0 = k \times \frac{NL}{Mp}$ elements, if $k \times n_0 = k \times \frac{NL}{Mp}$ is not an integer, a rounding cyclic shift $k \times n_0 = \lfloor k \times \frac{NL}{Mp} \rfloor$ takes place. The integer cyclic shift can be done by left column cyclic shift of sparse conversion matrix with $d = \lfloor k \times \frac{NL}{Mp} \rfloor$ columns, then the new sparse conversion matrix is defined as

$$\mathbf{S}_u = [\mathbf{t}_u^{(0+d)}, \mathbf{t}_u^{(1+d)}, \dots, \mathbf{t}_u^{(NL-1+d)}] \quad (4.27)$$

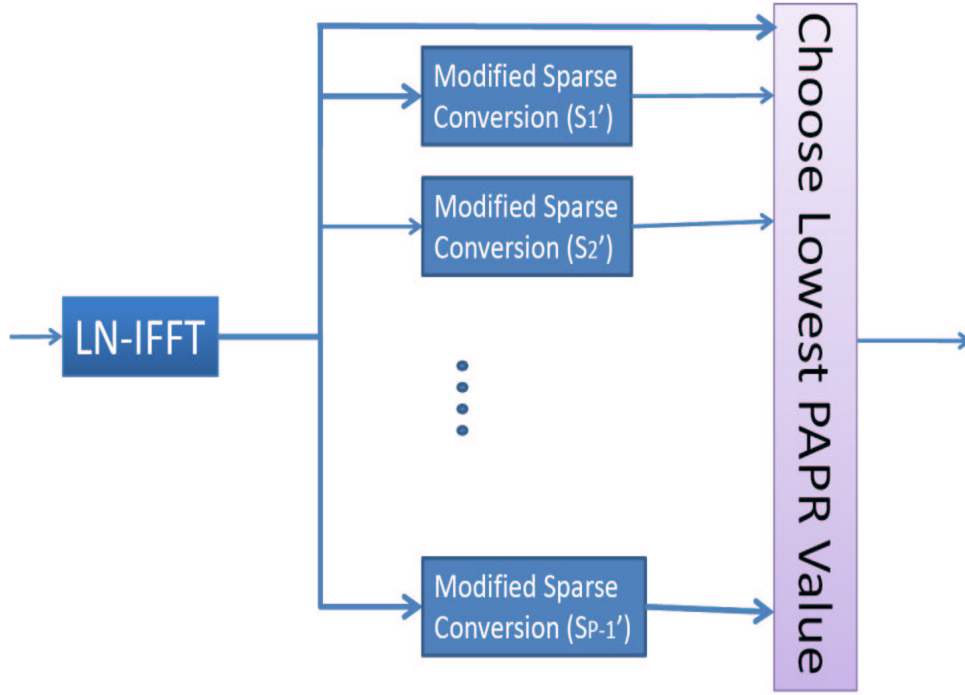


Figure 4.5: Block diagram of modified low complexity SLM encoder.

where $d = \lfloor k \times \frac{NL}{Mp} \rfloor$ defines the integer part of cyclic shift and $\mathbf{t}_u^{(k)}$ is the circularly down-shifted version of the column vector $\mathbf{t}_u^{(0)}$ by k elements.

4.7 Simulation Results

In this section we provide some numerical results of our sequence design. We consider an OFDM system with 256 sub-carriers using QPSK modulation for the data carried on $N = 160$ available subcarrier and it is operated under frequency selective channel. Since number of carriers is 160, group with order $p = 17$ shall be used. Each subgroup of $\mathbf{S}(g_k)$, $k = 1, \dots, p - 1$ forms sequence have to be repeated 10 times and \mathbf{u}_k is set to be uncorrelated. In addition, there is an all one sequence \mathbf{s}_0 which means that data encoded that sequence is equal to original data sequence \mathbf{x} .

In this chapter, random generated sequences and chaotic sequence [12] are used to compare with proposed sequence design. Most widely used chaotic logistic map presented

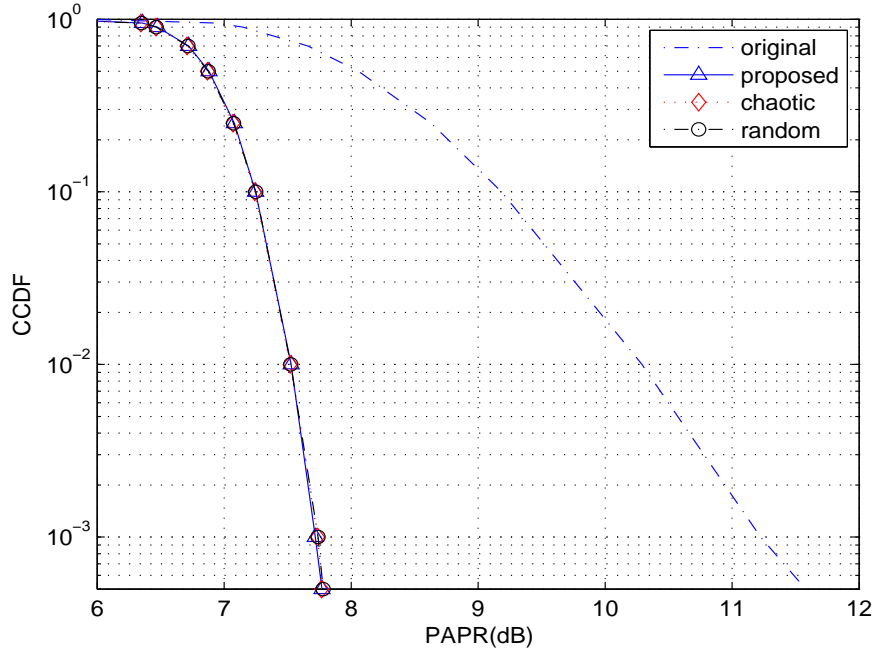


Figure 4.6: CCDF plot of PAPR performance of random sequences, chaotic sequences, and proposed sequences design.

in [12] is:

$$x_{n+1} = rx_n(1 - x_n), \quad 0 \leq x_n < 1, 0 \leq r \leq 4 \quad (4.28)$$

and r is called the bifurcation parameter. The outcome of chaotic generator is distributed in $[0, 1]$ with good correlation properties, and the sequence is mapped from x_n by the following function:

$$s_c(n) = e^{j2\pi x_n}, \quad n = 1, 2, \dots, 160 \quad (4.29)$$

Random generated sequences can be generated by mapping the random variable x_n which is uniformly distributed in $[0, 1]$ using the same mapping function in (4.29).

PAPR reduction performance has been proved to be proportional to the number of SLM sequences as long as SLM sequences are uncorrelated ([9] and [13]). Fig. 4.6 shows that any sequence design which has the same number of uncorrelated sequences will have the same PAPR performance. However, sequence index detection probability, which is called key error rate (KER) here, can be improved by well-designed sequences, and the

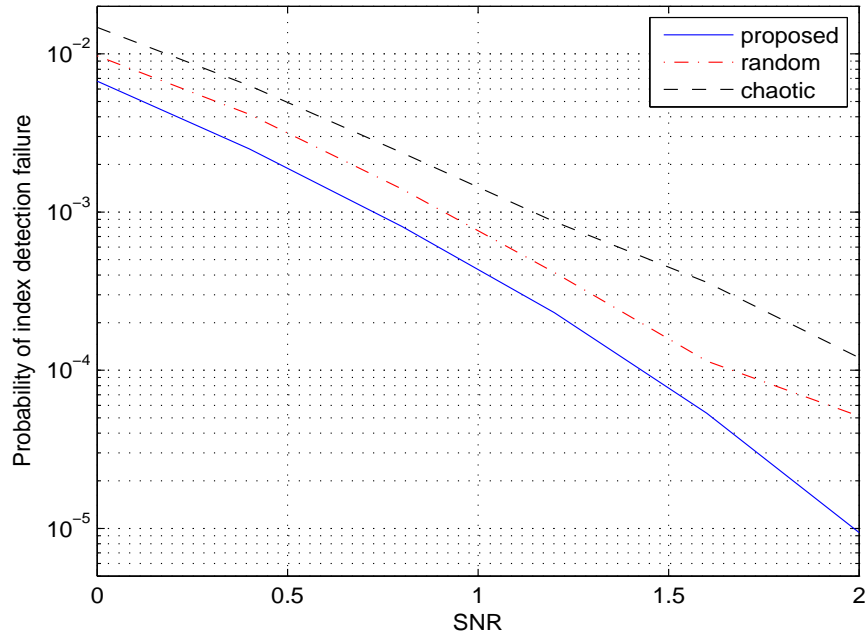


Figure 4.7: Probability of sequence index detection failure under frequency selective channel.

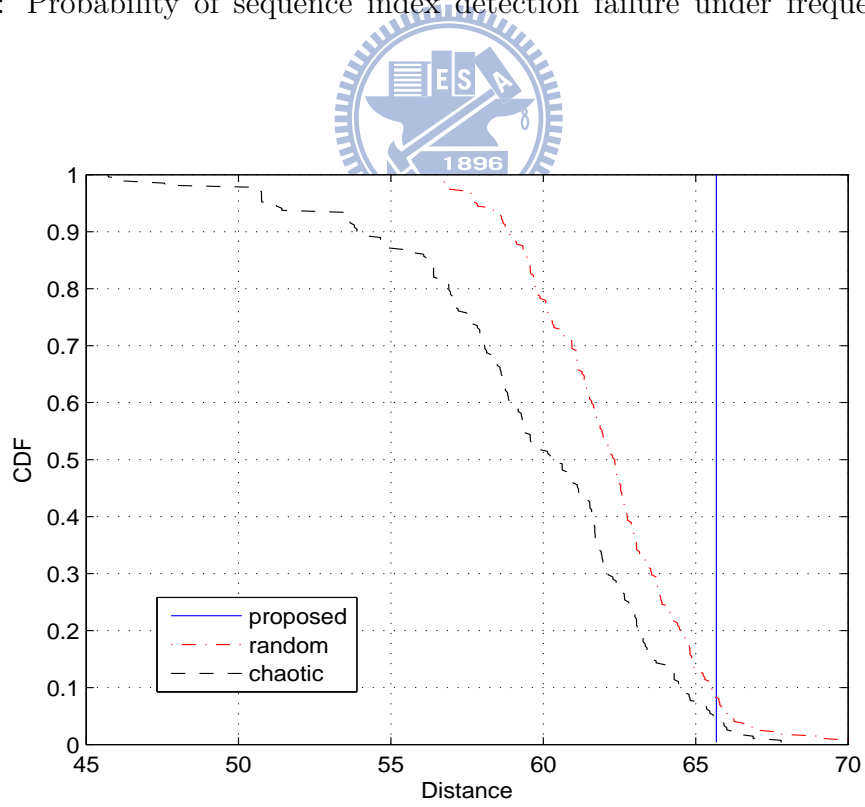


Figure 4.8: Euclidean distance of random sequences, chaotic sequences, and proposed sequence design.

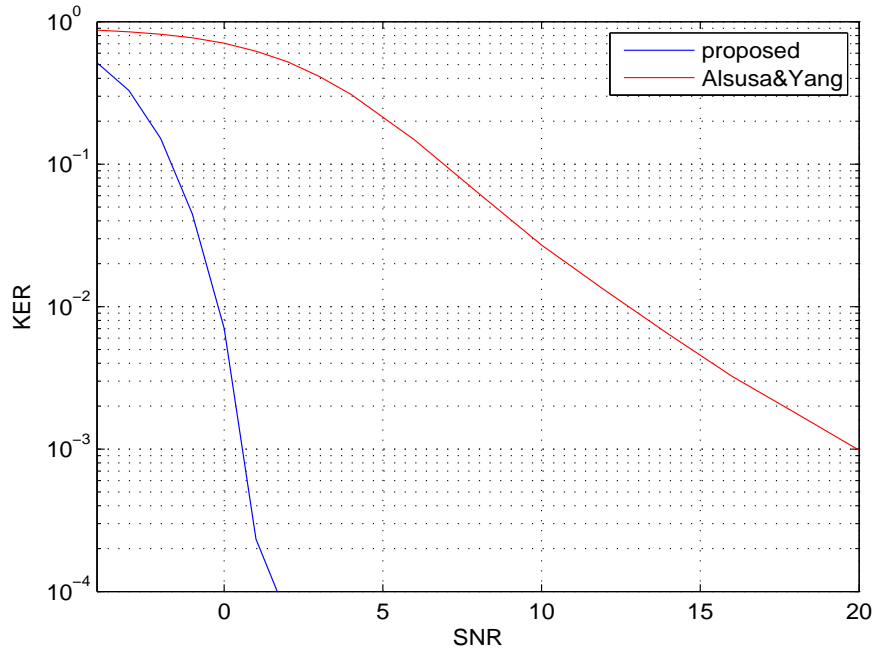


Figure 4.9: Probability of sequence index detection failure of proposed sequences and Alsusa and Yang sequences under frequency selective channel.

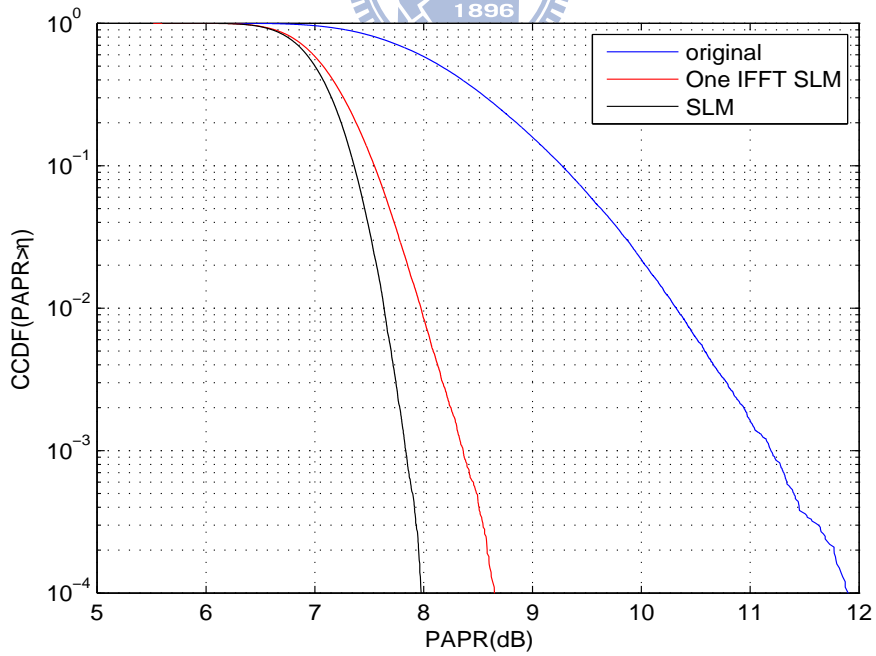


Figure 4.10: CCDF of PAPR performance of original OFDM symbol, low complexity SLM encoder, and original SLM.

proposed sequence design provides a promising coding gain that every sequence is $\frac{ND_{avg}}{p-1}$ far away from other sequences where $\frac{N}{p-1}$ have to be integer.

Fig. 4.8 shows the minimum pairwise distance of random generated sequences, chaotic sequences, and proposed sequence design. The minimum pairwise distance of random generated and chaotic sequences are much less than the minimum pairwise distance of proposed sequence design. As we can see in equation (4.15) that minimum distance would dominate performance of blind decoder. Fig. 5.7 shows the trend of this hypothesis and an asymptotically 0.3dB gain of proposed sequences to random and chaotic sequences for signal-to-noise ratio (SNR) larger than 1.5dB. Besides, our design criterion is to make all pairwise distance to be equal, and fig. 4.8 also shows that our design satisfy this criterion.

Alsusa and Yang [11] proposed an SLM sequences design in the proceedings of ICC 2006. Their design uses the locations of unmodified elements to identify different sequences, thus receiver has only to detect the locations of unmodified block. Their sequences have unmodified elements which is $e^{j0} = 1$ and other entries with magnitude 1 and phase $[0, 2\pi)$ distributed. In fig. 4.9, we can see that proposed design outperforms Alsusa and Wang's, since their design only use part of sequence to identify each SLM sequence. Sequence pattern of proposed design spread through whole sequence, hence full degree of freedom is employed for sequence detection.

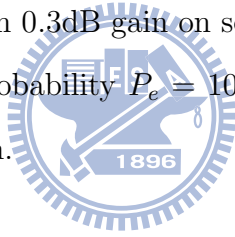
The proposed low complexity SLM encoder has only one IFFT operation, but it has PAPR loss since sparse conversion block has correlation in frequency domain. Although low complexity SLM encoder has 0.8dB PAPR loss at $CCDF = 10^4$ in fig. 4.10, the complexity is decreased from $O(LN \log(LN))$ to $O(4LN)$. While using SLM to be PAPR reduction scheme, the SLM sequences have to be stored in both transmitter and receiver sides to do the encoding and decoding. Only the data scrambling vectors \mathbf{u}_k , $k = 1, \dots, p-1$ have to be stored for using proposed sequences. It costs $\log_2 M$ bits of memory for one entry to store the vectors \mathbf{u}_k . In the case of QPSK, 2 bits memory for

one element in sequence is needed.

The SLM scheme is simple, quick and effective in the sense of reducing PAPR; however, SLM is not recommended in several latest released standard proposals due to its sequence index detection failure. Since we can achieve the sequence detection failure probability $Pe = 10^{-5}$ at 2dB SNR which is acceptable in wireless communication, SLM should be reconsidered to be a main PAPR reduction scheme.

4.8 Chapter Summary

In this chapter, a novel selective mapping sequence design is proposed that minimum pairwise distance of arbitrary two sequences is equal. It provides the system a bound of minimum distance D_{avg} between sequences which has a guaranteed coding gain that every codeword is separated at least D_{avg} apart. And simulation results show that proposed design scheme has more than 0.3dB gain on sequence index detection probability and it reaches detection failure probability $P_e = 10^{-5}$ at $SNR = 2\text{dB}$ which is robust enough for wireless communication.



Chapter 5

Selective Mapping with Embedded Side Information

In this chapter, we present an improved non-blind SLM-based PAPR reduction scheme which uses SLM as the main PAPR reduction mechanism; side information (SI) is transmitted within the same OFDM symbol. The embedded SI is further exploited to reduce PAPR and enhance SI detection performance.

5.1 System Model

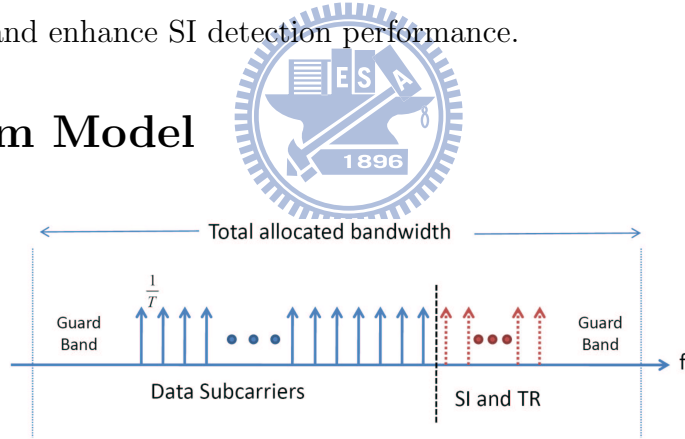


Figure 5.1: Bandwidth utilization of proposed scheme.

We consider an OFDM system with N in-band sub-carriers which can be divided into data sub-carriers set $S_d = \{l_{d_0}, \dots, l_{d_{D-1}}\}$ with cardinality D and SI sub-carriers set $S_I = \{l_{I_0}, \dots, l_{I_{P-1}}\}$ with cardinality P . $\mathbf{X} = [X[l_{d_0}], \dots, X[l_{d_{D-1}}]]$ is data vector which is modulated by quadrature amplitude modulation (QAM). SLM sequence denotes as $\mathbf{s}_{\mathbf{u}}\mathbf{k} = [\mathbf{S}_{\mathbf{k}}[l_{d_0}], \dots, \mathbf{s}_{\mathbf{u}}[l_{d_{D-1}}]]$ and each entry is uniformly distributed in $[0, 2\pi)$ and $u \in \mathbb{K}$ with cardinality $|\mathbb{K}| = U$. Given the original OFDM symbol, U alternative representa-

tions of signal candidates, $\hat{\mathbf{X}}_u = \mathbf{X} \odot \mathbf{s}_u$, can be obtained by element-wise multiplying the original OFDM symbol with different SLM sequences. Furthermore, the SI of SLM sequence, which is the index of the used sequence, is modulated onto sub-carriers of S_I . The SI vector denotes as $\mathbf{A}_{si}^u = [A_{si}^u[l_{I_0}], \dots, A_{si}^u[l_{I_{P-1}}]]$. The entire frequency domain OFDM symbol can be represented as $\tilde{\mathbf{X}}_u = [\hat{X}_u[l_{d_0}], \dots, \hat{X}_u[l_{d_{D-1}}], A_{si}^u[l_{I_0}], \dots, A_{si}^u[l_{I_{P-1}}]]$ which is the scrambled data plus embedded SI.

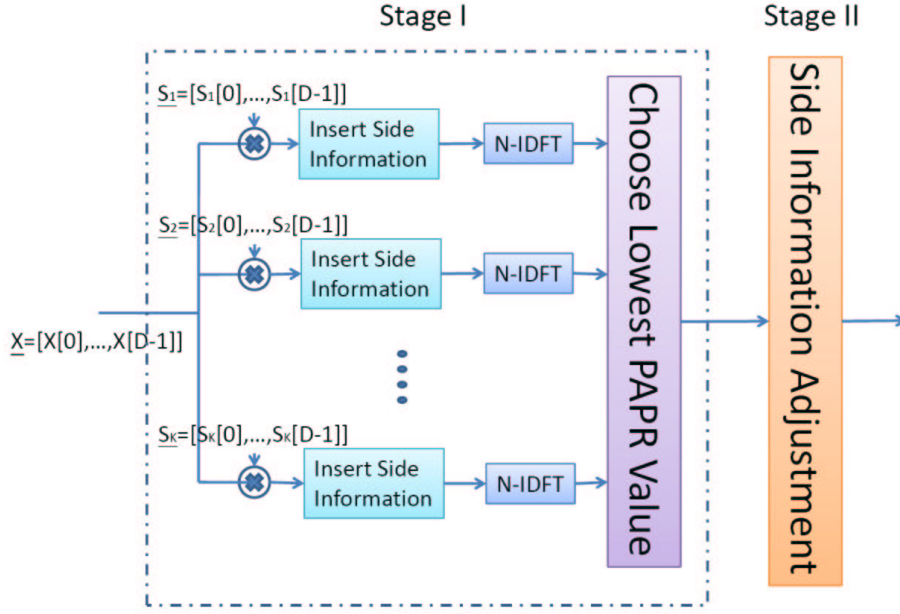


Figure 5.2: Original SLM encoder with embedded SI.

Our scheme consists of two stages. In the first stage, we choose the one with lowest PAPR among U different candidate SLM-encoded OFDM symbols. Second stage adopts two different algorithms to reduce PAPR by adjusting the SI symbols meanwhile having better SI detection error protection. The first algorithm employs active constellation extension (ACE) [4] to adjust SI and the second algorithm uses POCS [15] for SI adjustment.

This chapter is organized as follow: Section II consider the encoding and insertion of SI, ACE and POCS are introduced in section III. Simulation results and brief conclusion are provided in section IV and V.

5.2 Encoding Side Information and Insertion

5.2.1 Insertion of the Side Information

The main concern of using SLM scheme is the correctness of SI, and channel coding techniques are involved for having better error protection. Original SI bits are $\log_2(U)$ and the encoded SI bits are $\log_2(n)$ if (n,k) linear block code is used. And the number of SI sub-carriers can be determined by the ratio of encoded SI bits and modulation type of SI sub-carriers.

$$P = \lceil \frac{n}{\log_2(M)} \rceil \quad (5.1)$$

where M is the number of constellation points of the modulation type being used. The vector representing SI symbols is generated by a mapping S which maps the index u to a vector of QAM symbol \mathbf{A}_{si}^u

$$S: u \rightarrow \mathbf{A}_{si}^u, u = 1, \dots, U \quad (5.2)$$

and the index of \mathbf{A}_{si}^u can be seen in figure 5.1.

5.2.2 Estimation of Side Information

At the receiver, after applying discrete fourier transform (DFT) and zero-forcing equalization the received OFDM frequency symbol is denoted as \mathbf{Y} and SI vector is denoted as \mathbf{Y}_{si} . The noisy vector \mathbf{Y}_{si} consists of signal apart \mathbf{A}_{si}^u and noise part with variance $\sigma_n^2/|H_n|^2$.

Maximum likelihood (ML) estimation is applied for decoding sequence index u . The estimate \hat{u} can be obtained by

$$\begin{aligned} \hat{u} &= \arg \max_{u=1, \dots, U} \{Pr\{\mathbf{Y}_{si} | \mathbf{A}_{si}^u\}\} \\ &= \arg \max_{u=1, \dots, U} \left\{ \prod_{n=0}^{P-1} Pr\{Y_{si}[n] | A_{si}^u[n]\} \right\} \\ &= \arg \min_{u=1, \dots, U} \left\{ \sum_{n=0}^{P-1} \frac{|Y_{si}[n] - A_{si}^u[n]|^2}{\sigma_n^2/|H_n|^2} \right\} \end{aligned} \quad (5.3)$$

In order to execute the ML estimator channel state information $|H_n|^2$ and noise variance σ_n^2 have to be known.

5.2.3 Encoding Scheme of SI

Several earlier approaches [16] use (7,4) Hamming code to encode SI.

Example: The number of SLM sequences in the set \mathbf{K} is 16, so we can use the 3-bit representation $\{(0, 0, 0, 0), (0, 0, 0, 1), \dots, (1, 1, 1, 1)\}$ for the sequence index. Using the Hamming code with generator matrix G given by

$$G = \begin{pmatrix} 1 & 1 & 0 & 1 \\ 1 & 0 & 1 & 1 \\ 1 & 0 & 0 & 0 \\ 0 & 1 & 1 & 1 \\ 0 & 1 & 0 & 0 \\ 0 & 0 & 1 & 0 \\ 0 & 0 & 0 & 1 \end{pmatrix} \quad (5.4)$$

we obtain 7-bit encoded vectors by $\mathbf{c} = \mathbf{u}G$.

Since ML estimation is used for decoding sequence index, only generator matrix or generator polynomial is needed for transmitter and receiver.

For proposed scheme, BCH code is involved for a better error protection capability. One of the advantages of BCH is easy implementation that shift register can be used to generate encoding sequence. Polynomial representation for information bits and generator polynomial is needed. For BCH(31,6,7), information bits should be written as $\{X, X+1, \dots, X^5 + X^4 + X^3 + X^2 + X + 1\}$ and the generator polynomial is

$$g(X) = X^{25} + X^{24} + X^{21} + X^{19} + X^{18} + X^{16} + X^{15} + X^{14} + X^{13} + X^{11} + X^9 + X^5 + X^2 + X + 1 \quad (5.5)$$

The resulting encoded sequence is denoted as $\mathbf{c}^u = [c^u[0], \dots, c^u[31-1]]$.

As we have no posterior information of the peak locations of time domain SLM encoded signal, the PAPR of SI vector should be minimized. If the number of SI bits ($\log_2(U)$) are less than that of the input information bits (k), there is extra degrees of freedom can be used to find SI with smaller PAPR. In proposed scheme, the number

of SLM sequences is $U = 8$ and the (31,6,7) BCH code is used to encode SI. Hence, we choose the eighth lowest PAPR sequences among all the possible encoded BCH sequences. It shall be mentioned that this process shall include the modulation of encoded bits onto SI sub-carriers and the results will be different if the modulation scheme is different.

5.3 Side Information Adjustment Algorithm

Our scheme is a two-stage algorithm (see Fig. 5.2) whose first stage involves the insertion of SI and the selection among possible candidate SLM-encoded vectors. This section discusses the second stage operations where clipping is employed while frequency domain feasible set is defined on SI sub-carriers only. There are two algorithm being adopted.

5.3.1 Problem Formulation

The effect of inserted SI can be viewed as a time domain signal $\mathbf{a}_u = IDFT\{\mathbf{A}_{si}^u\}$, which is contributed by SI only, plus the time domain SLM encoded signal $\hat{\mathbf{x}} = IDFT\{\hat{\mathbf{X}}\}$. And the addition of the two signals should be minimized below threshold η . This can be formed as an optimization problem

$$\begin{aligned}
 & \min \quad \eta \\
 & \text{s.t} \\
 & \quad \|\tilde{\mathbf{x}}\|_{\infty} \leq \eta \\
 & \quad \text{where } \tilde{\mathbf{a}}_u = IDFT\{\mathbf{A}_{si}^u + \mathbf{e}_{si}\} \\
 & \quad \hat{\mathbf{x}} = IDFT\{\hat{\mathbf{X}}\} \\
 & \quad \|\tilde{\mathbf{x}}\|_{\infty} = \|\hat{\mathbf{x}} + \tilde{\mathbf{a}}_u\|_{\infty} \\
 & \text{in variables : } \mathbf{e}_{si} \in \mathbb{C}^{NL}, \eta \in \mathbb{R}
 \end{aligned} \tag{5.6}$$

SLM encoded signal $\hat{\mathbf{x}} = IDFT\{\hat{\mathbf{X}}\}$ shall not be changed to maintain the bit error rate (BER) performance, thus only SI part $\tilde{\mathbf{a}}_u$ can be modified to reduce PAPR. There are two algorithms, active constellation extension (ACE) and projection onto complex set (POCS), can be adopted, and they will be introduced in the following two subsections.

5.3.2 Active Constellation Extension for SI Adjustment

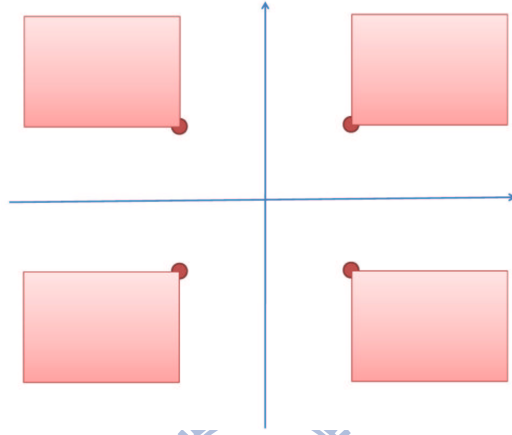


Figure 5.3: Extended region of QPSK denoted as F .

The encoded SI vector is binary, and quadrature phase shift keying (QPSK) is used as the mapping S from sequence index u to SI vector \mathbf{A}_{si}^u . Thus the number of SI subcarriers can be determined by $\lceil \frac{n}{\log_2(4)} \rceil$. ACE algorithm is used to modified \mathbf{A}_{si}^u within the frequency domain constraint set. By doing so, the PAPR of the modified symbol will be reduced and as the constellation points are further apart from decision boundary, the detection error protection is improved. Here, we define frequency domain extended region as feasible set F for modified SI symbol in figure 5.3.

The new PAPR reduction problem can be written as follow:

$$\begin{aligned}
& \min \quad \eta \\
& \text{s.t.} \\
& \quad \|\tilde{\mathbf{x}}\|_{\infty} \leq \eta \\
& \quad \text{where } \tilde{\mathbf{a}}_u = IDFT\{\mathbf{A}_{si}^u + \mathbf{e}_{si}\} \\
& \quad \hat{\mathbf{x}} = IDFT\{\hat{\mathbf{X}}\} \\
& \quad \|\tilde{\mathbf{x}}\|_{\infty} = \|\hat{\mathbf{x}} + \tilde{\mathbf{a}}_u\|_{\infty} \\
& \quad \text{in variables : } \mathbf{e}_{si} \in \mathbb{C}^{NL}, \eta \in \mathbb{R}
\end{aligned} \tag{5.7}$$

One simple way is iterative clipping and filtering that the time domain signal is first clipped and followed by restoring data vector back to its original value of the SLM encoder output and projecting the SI symbol back to frequency domain feasible set F . The iterative signal update can be written as

$$\tilde{\mathbf{x}}^{i+1} = \tilde{\mathbf{x}}^i + \mu \mathbf{e}^i \tag{5.8}$$

where i is the iteration number, and \tilde{x}^i is the time domain iterative signal. The clipping rule is

$$\begin{aligned}
Re\{\bar{x}[n]\} &= \begin{cases} Re\{\tilde{x}^i[n]\}, & |Re\{\tilde{x}^i[n]\}| \leq \eta; \\ \eta, & |Re\{\tilde{x}^i[n]\}| > \eta \end{cases} \\
Im\{\bar{x}[n]\} &= \begin{cases} Im\{\tilde{x}^i[n]\}, & |Im\{\tilde{x}^i[n]\}| \leq \eta; \\ \eta, & |Im\{\tilde{x}^i[n]\}| > \eta \end{cases} \\
\bar{\mathbf{x}} &= Re\{\bar{\mathbf{x}}\} + j * Im\{\bar{\mathbf{x}}\}
\end{aligned} \tag{5.9}$$

Thus, the time domain error vector is $\mathbf{e}_{clip}^i = \bar{\mathbf{x}} - \tilde{\mathbf{x}}^i$ and the frequency domain error vector can be obtained by $\mathbf{E}_{clip}^i = DFT\{\mathbf{e}_{clip}^i\}$. And the frequency update signal \mathbf{E}^i has to satisfy several predefined frequency domain constraint that error at data part should be zero $E^i[n] = 0, n = l_{d_0}, \dots, l_{d_{D-1}}$ and error at SI has to be within frequency feasible set

$$E^i[n] = \begin{cases} E^i[n] = E_{clip}[n], & n = l_{I_0}, \dots, l_{I_{P-1}}, \text{ if } E_{clip}[n] \in E; \\ E^i[n] = proj(E_{clip}[n], E), & n = l_{I_0}, \dots, l_{I_{P-1}}, \text{ otherwise} \end{cases}$$

where $proj(a, A)$ is the function that project a onto the nearest point in set A . And the time domain update signal is $\mathbf{e}^i = IDFT\{\mathbf{E}^i\}$.

Jones [4] introduces smart gradient projection (SGP) algorithm that step size μ is updated for every iteration. The ACE-SGP algorithm is list as follow:

Step 1:	Initialization: Set iteration number $i = 0$, and clipping threshold η
Step 2:	$\bar{\mathbf{x}}$ is obtained by clipping $\tilde{\mathbf{x}}^i$ with threshold η . Compute the update signal of $\mathbf{e}^i[n]$ by $\mathbf{e}_{clip}^i = \bar{\mathbf{x}} - \tilde{\mathbf{x}}^i$. and compute projection of $e^i[n]$ along $\tilde{x}^i[n]$ for every sample. $e_{proj}[n] = \frac{\Re\{\tilde{x}^i[n] * e^{i*}[n]\}}{ \tilde{x}^i[n] }$, $n = 0, \dots, N - 1$
Step 3:	Given $\tilde{\mathbf{x}}^i$, compute maximum magnitude E and the corresponding sample position n_{max} for iteration i $P = \max_n \tilde{x}^i[n] $ $n_{max} = \arg \max_n \tilde{x}^i[n] $
Step 4:	Compute approximate balancing for $e_{proj}[n] > 0$ $\mu[n] = \frac{P - \tilde{x}^i[n] }{e_{proj}[n] - e_{proj}[n_{max}]}$. Choose the minimum μ as step size.
Step 5:	Update the signal $\mathbf{x}^{i+1} = \mathbf{x}^i + \mu \mathbf{e}^i$ with variable step size μ .
Step 6:	Iteratively execute from step 2 to step 5. If μ is negative, stop algorithm.

Table 5.1: Active constellation extension with smart gradient projection algorithm.

Usually, the SGP algorithm converges to a near-optimal solution within 5 iterations. As we can see, the feasible set of ACE algorithm is only in a quadrant which means the phase of SI symbol can only be changed from $-\frac{\pi}{4}$ to $\frac{\pi}{4}$. In the following, we come up with an idea to have phase of SI symbol to change from 0 to 2π , and the phase degree of freedom is employed. And this is introduced next for AM modulation of SI vector.

5.3.3 Projection onto Complex Set for SI Adjustment

Since phase degree of freedom of SI symbol is concerned, SI symbol should be freely moved from 0 to 2π and carry information on amplitude. Thus, the mapping rule $S : u \rightarrow \mathbf{A}_{si}^u$ is amplitude modulation which maps 0 onto unit circle and 1 onto circle with radius 2. And the number of SI sub-carriers can be determined by $\lceil \frac{n}{\log_2(2)} \rceil = n$. The mapping S is

$$A_{si}^u[i] = \begin{cases} 1 \cdot e^{j\theta[i]}, & \text{if } c^u[i] = 0; \\ 2 \cdot e^{j\theta[i]}, & \text{if } c^u[i] = 1 \end{cases}$$

where phase $\theta[i]$, $i = 0, \dots, n-1$ is uniformly distributed in $[0, 2\pi)$. The frequency domain feasible set C is defined in figure 5.4.

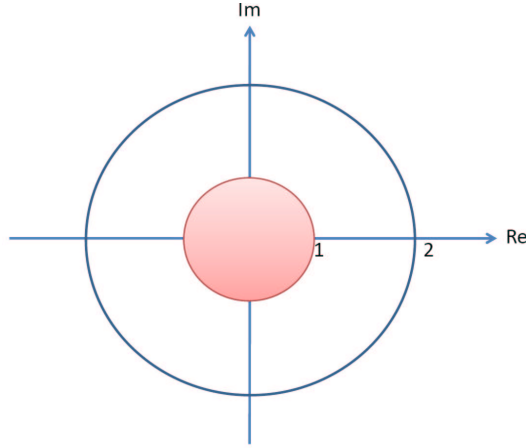


Figure 5.4: Amplitude modulation for POCS algorithm.

And the PAPR reduction problem becomes:

$$\begin{aligned}
& \min \quad \eta \\
& \text{s.t.} \\
& \quad \|\tilde{\mathbf{x}}\|_{\infty} \leq \eta \\
& \quad |A_{si}^u[i]| \leq 1, \text{ if } c^u[i] = 0 \\
& \quad |A_{si}^u[i]| \geq 2, \text{ if } c^u[i] = 1 \\
& \text{where } \tilde{\mathbf{a}}_u = \text{IDFT}\{\mathbf{A}_{si}^u + \mathbf{e}_{si}\} \\
& \quad \hat{\mathbf{x}} = \text{IDFT}\{\hat{\mathbf{X}}\} \\
& \quad \|\tilde{\mathbf{x}}\|_{\infty} = \|\hat{\mathbf{x}} + \tilde{\mathbf{a}}_u\|_{\infty} \\
& \text{in variables : } \mathbf{e}_{si} \in \mathbb{C}^{NL}, \eta \in \mathbb{R}
\end{aligned} \tag{5.10}$$

As we can see in fig. 5.4. that the outer circle is not a convex set, and it can not be solved by any convex optimization tool, thus projection onto complex set algorithm is a sub-optimal algorithm to take place. The following is POCS algorithm:

Step 1:	Initialization vector $\tilde{\mathbf{x}}$ is IDFT of $\tilde{\mathbf{X}}$.
Step 2:	Enforce $\tilde{\mathbf{x}}$ to satisfy the pre-defined threshold η . If the modified $\bar{\mathbf{x}}$ satisfies $\bar{\mathbf{x}} = \tilde{\mathbf{x}}$, then terminated. Otherwise, go to step 3.
Step 3:	Perform DFT to $\bar{\mathbf{x}}$ to obtain $\bar{\mathbf{X}}$, and restore data part $[\bar{X}[l_{d_0}], \dots, \bar{X}[l_{d_{D-1}}]] = \hat{\mathbf{X}}$ and project SI part $[proj(\bar{X}[l_{I_0}], C), \dots, proj(\bar{X}[l_{I_{P-1}}], C)]$ to the closest point in C .
Step 4:	Iteratively execute step 2 and step 3 until there is no PAPR reduction gain or PAPR is small enough.

Table 5.2: Projection onto Complex Set algorithm.

Next section, simulation results are provided, and modified SI symbols by ACE algorithm and POCS algorithm is observed.

5.4 Numerical Results

In this section, we provide several numerical results to show the key error rate (KER) which is the SI detection probability and CCDF of PAPR performance. Also, the figures of modified frequency domain SI is provided. For different SI modulation we have different settings to make them comparable. For QPSK modulation of SI, an OFDM symbol with 256 sub-carriers is considered, and 152 in-band sub-carriers are further divided into 136 data sub-carriers and 16 SI sub-carriers. However, for AM modulation of SI, an OFDM symbol with 512 sub-carriers is considered, and 304 in-band sub-carriers are further divided into 273 data sub-carriers and 31 SI sub-carriers. Thus, the ratio of SI sub-carriers and total sub-carriers are equal for both system. The number of SLM sequences is 8 and BCH(31,6,7) is used for SI encoding. The system is simulated under frequency selective channel for error rate performance.

First, we would like to show the modified SI do locate inside the defined frequency domain constraint set. In fig. 5.5., the modified SI do stay within the extended region, and the red cross stands for original QPSK constellation points and blue circle means the modified symbol. In fig. 5.6, $r = 1$ red circle stands for the amplitude modulation for information bit 0 and $r = 2$ red circle stands for the amplitude modulation for information bit 1. The symbols do stay within the constraint set with random phase. For both scheme, symbols move opposite direction toward decision boundary, thus SI detection probability is improved.

The simulated KER and PAPR performance are provided in fig. 5.7, fig. 4.6 In Fig. 4.6, the POCS algorithm and ACE algorithm can further reduce PAPR than original SLM and SLM with inserted SI. POCS outperform ACE because POCS has more phase degree of freedom than ACE. As we can see from the constraint set of ACE (Fig. 5.3),

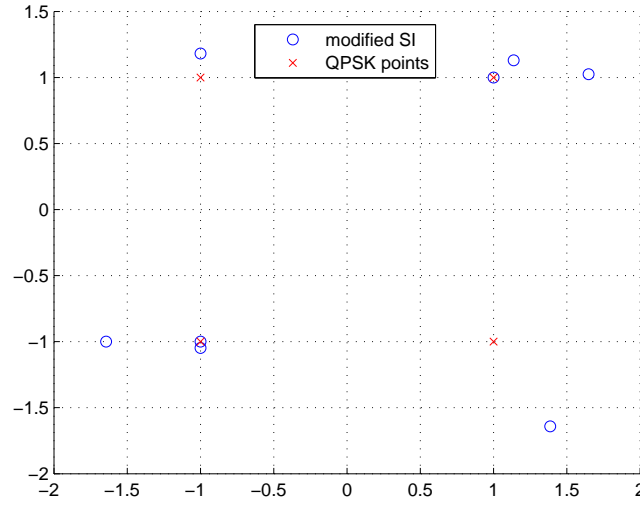


Figure 5.5: Location of modified SI symbol using active constellation extension (ACE) algorithm.

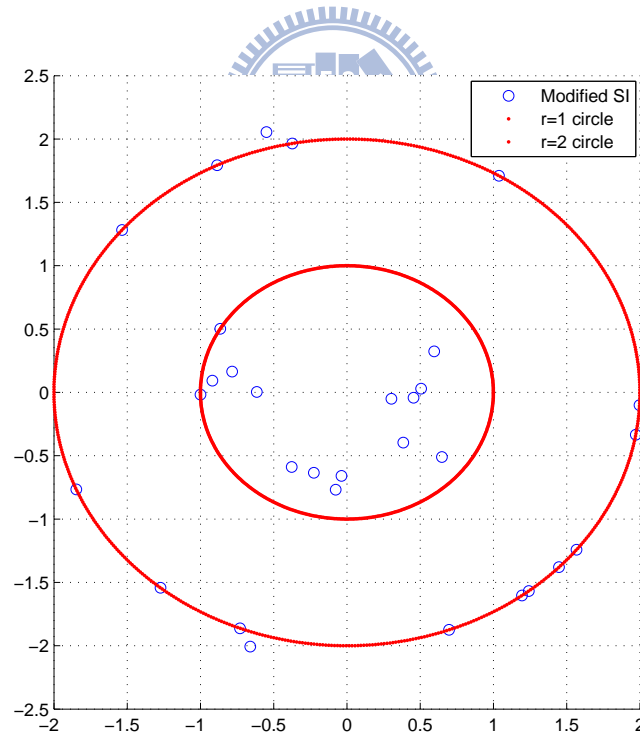


Figure 5.6: Location of modified SI symbol using projection onto complex set (POCS) algorithm.

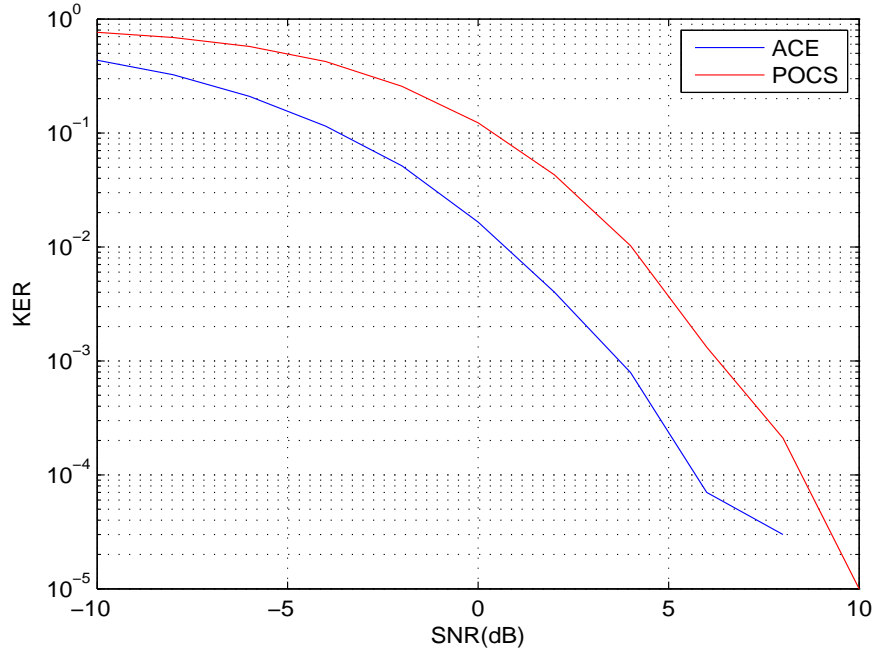


Figure 5.7: Key error rate for ACE and POCS schemes.

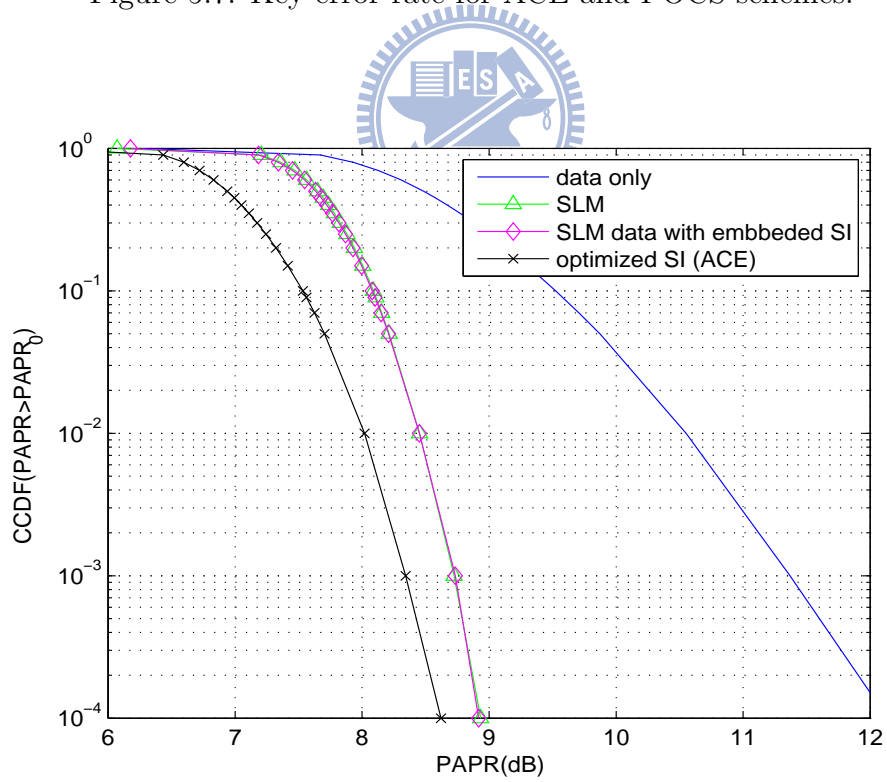


Figure 5.8: CCDF of PAPR of original SLM, SLM embedded SI, and SLM with modified SI (ACE).

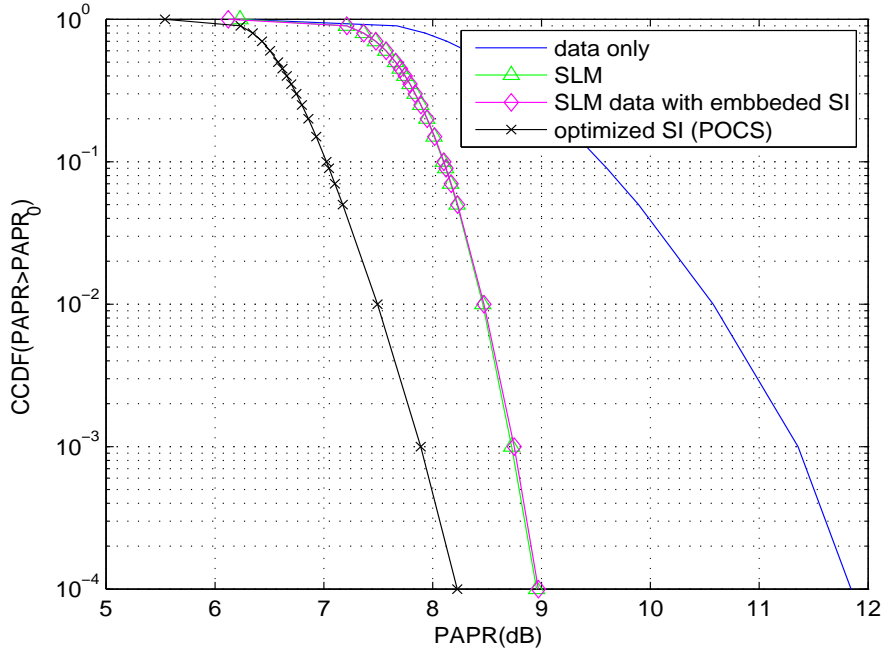


Figure 5.9: CCDF of PAPR of original SLM, SLM embedded SI, and SLM with modified SI (POCS).

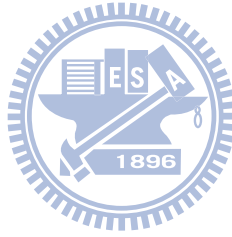
the phase degree of freedom for every symbol is $[-\pi/4, \pi/4]$; however, for constraint set of POCs (Fig. 5.4), every symbol has phase degree of freedom from $[0, 2\pi)$. It is believed that phase degree of freedom is much more effective than magnitude degree of freedom in the sense of PAPR reduction.

Fig. 5.7. shows that there is a 3dB KER performance gap between ACE and POCS schemes, because the minimum distance of QPSK constellation is twice the minimum distance of Amplitude modulation, and also ML symbol-wise estimation is used. Despite of the 3dB gap, the KER decreases to 10^{-4} at SNR=5 (ACE) and SNR=8 (POCS). Such performance is robust enough for wireless communication.

5.5 Chapter Summary

In this chapter, we provide another option for SI transmission to receiver that SI is inserted within the same OFDM symbol. Two algorithms are proposed to modified

SI to further reduce PAPR. Simulation results show that with second stage cascaded, PAPR reduction outperforms than original SLM and it reaches KER $Pe = 10^{-4}$ at 5dB and 8dB SNR for ACE and POCS, respectively.



Chapter 6

Conclusion

6.1 Summary of Contributions

Peak-to-average power ratio is one of the most critical design concerns for OFDM systems. We have presented two new PAPR reduction approaches and a SLM sequence design in this thesis.

We first proposed a nonlinear clipping method with hybrid frequency domain constraints to obtain a larger feasible set. The PAPR reduction problem is formulated as a standard linear programming (LP) form which can then be solved by well-developed LP tools to obtain the optimal clipping threshold and optimal clipped OFDM symbols.

A novel SLM sequences design aimed to offer improved blind (non-side-information aided) detection performance is proposed. Our design renders a simple hardware realization with less memory requirement.

Our third contribution has to do with side information transmission in an SLM system. Our scheme inserts the SI in the same OFDM symbol. By adjusting SI we further reduce the PAPR. ACE and POCS algorithms are adopted to modify the transmitted SI.

6.2 Some Future Works

The complexity of the LP solution presented is still high for real-time implementation. Better algorithms are needed to reduce the overall the complexity of solving the target LP problem. Finding a mathematical connection between error vector magnitude and bit error rate performance remains unsolved. If such a relationship can be established then one can solve the PAPR reduction and BER minimization simultaneously.

For the SLM-aided OFDM system, we believe that both the associated blind decoder complexity and performance can be further improved. Analysis of the exact blind sequence detection probability and the corresponding BER performance is also desired.

For the proposed SI-aided scheme to become practical, we have to reduce the required number of SI sub-carriers to improve bandwidth efficiency. Further complexity suggestions are always welcome. Linear system with sparse solution optimization problem might be needed to find a near-optimal solution for projection onto convex set algorithm.



Appendix

In this Appendix, we continue on proving that minimum pairwise distance of any two arbitrary sequences are equal. Here we have three arbitrary sequences

$$D(\mathbf{S}(g_1)) = D([W_{Mp}^{k_1}, W_{Mp}^{2k_1}, \dots, W_{Mp}^{(p-1)k_1}] \otimes \mathbb{D}) \quad (6.1)$$

$$= [W_{Mp}^{(k_1 \bmod p)}, W_{Mp}^{(2k_1 \bmod p)}, \dots, W_{Mp}^{((p-1)k_1 \bmod p)}] \quad (6.2)$$

$$k_1 \in [0, p-1] \in \mathbb{Z}$$

$$D(\mathbf{S}(g_2)) = D([W_{Mp}^{k_2}, W_{Mp}^{2k_2}, \dots, W_{Mp}^{(p-1)k_2}] \otimes \mathbb{D}) \quad (6.3)$$

$$= [W_{Mp}^{(k_2 \bmod p)}, W_{Mp}^{(2k_2 \bmod p)}, \dots, W_{Mp}^{((p-1)k_2 \bmod p)}] \quad (6.4)$$

$$k_2 \in [0, p-1] - \{k_1\} \in \mathbb{Z}$$

$$D(\mathbf{S}(g_3)) = D([W_{Mp}^{k_3}, W_{Mp}^{2k_3}, \dots, W_{Mp}^{(p-1)k_3}] \otimes \mathbb{D}) \quad (6.5)$$

$$= [W_{Mp}^{(k_3 \bmod p)}, W_{Mp}^{(2k_3 \bmod p)}, \dots, W_{Mp}^{((p-1)k_3 \bmod p)}] \quad (6.6)$$

$$k_3 \in [0, p-1] - \{k_1, k_2\} \in \mathbb{Z}$$

where $D(\cdot)$ is the relative distance function of sequence to the nearest constellation points. Since relative distance to constellation points is considered, equation (6.1)(6.3)(6.5) and equation (6.2)(6.4)(6.6) can be seen as to calculate relative distance of those expression to nearest constellation points.

We now use predefined distance function $D(\mathbf{x}_1, \mathbf{x}_2)$ to calculate the pairwise relative distance between this three sequences. The relative distance between $\mathbf{S}(g_1)$ and $\mathbf{S}(g_2)$

can be calculate as

$$D(\mathbf{S}(g_1), \mathbf{S}(g_2)) = \sum_{n=0}^{p-1} \min |W_{Mp}^{k_1 n} \otimes \mathbb{D} - W_{Mp}^{k_2 n} \otimes \mathbb{D}|^2 \quad (6.7)$$

$$= \sum_{n=0}^{p-1} |W_{Mp}^{(k_1 n \bmod p)} - W_{Mp}^{(k_2 n \bmod p)}|^2 \quad (6.8)$$

$$= \sum_{n=0}^{p-1} |1 - W_{Mp}^{((k_2 - k_1)n \bmod p)}|^2 \quad (6.9)$$

In (6.7)–(6.8), we use $(\bmod p)$ to replace $(\otimes \mathbb{D})$ as in (6.1) and (6.2).

The relative distance between $\mathbf{S}(g_1)$ and $\mathbf{S}(g_3)$ can be calculate as

$$D(\mathbf{S}(g_1), \mathbf{S}(g_3)) = \sum_{n=0}^{p-1} \min |W_{Mp}^{k_1 n} \otimes \mathbb{D} - W_{Mp}^{k_3 n} \otimes \mathbb{D}|^2 \quad (6.10)$$

$$= \sum_{n=0}^{p-1} |W_{Mp}^{(k_1 n \bmod p)} - W_{Mp}^{(k_3 n \bmod p)}|^2 \quad (6.11)$$

$$= \sum_{n=0}^{p-1} |1 - W_{Mp}^{((k_3 - k_1)n \bmod p)}|^2 \quad (6.12)$$

(6.10) is simplified to be (6.11) in the same sense of (6.7) and (6.8).

However, $\mathbf{s}(g_k^n) = (W_{Mp}^{kn})$, $n = 1, \dots, p-1$ is character vector of group $S(p)$. Since p is odd prime number, it can be shown by (??) that

$$\mathbf{s}(g_1^n - g_2^n) = \mathbb{P} \mathbf{s}(g_1^n - g_3^n) \quad (6.13)$$

where \mathbb{P} is permutation matrix.

We can apply this relation to the distance function $D(\mathbf{x}_1, \mathbf{x}_2)$ since \mathbf{x}_1 and \mathbf{x}_2 have the relation in (6.13). The corresponding distance character of (6.9) and (6.12) are

$$\tilde{\mathbf{S}}_{21} = |1 - W_{Mp}^{((k_2 - k_1)n \bmod p)}|, \quad n = 1, \dots, p-1$$

$$\tilde{\mathbf{S}}_{31} = |1 - W_{Mp}^{((k_3 - k_1)n \bmod p)}|, \quad n = 1, \dots, p-1$$

will also satisfy the same relation that

$$\tilde{\mathbf{S}}_{21} = \mathbb{P} \tilde{\mathbf{S}}_{31}$$

where \mathbb{P} is permutation matrix. Therefore,

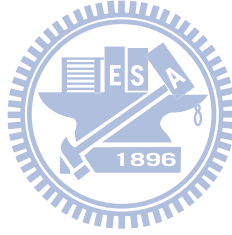
$$\begin{aligned} \sum_{n=0}^{p-1} |1 - W_{Mp}^{((k_3-k_1)n \bmod p)}|^2 &= \sum_{n=0}^{p-1} |1 - W_{Mp}^{((k_2-k_1)n \bmod p)}|^2 \\ D(\mathbf{S}(g_1), \mathbf{S}(g_2)) &= D(\mathbf{S}(g_1), \mathbf{S}(g_3)) \end{aligned} \quad (6.14)$$

and

$$\begin{aligned} D(\mathbf{S}(g_1), \mathbf{S}(g_2)) &= D(\mathbf{S}(g_2), \mathbf{S}(g_3)) \\ D(\mathbf{S}(g_1), \mathbf{S}(g_2)) &= d \\ D(\mathbf{S}(g_2), \mathbf{S}(g_3)) &= d \end{aligned} \quad (6.15)$$

$$(6.16)$$

which prove that arbitrary two sequences of proposed design have equal pairwise distance.

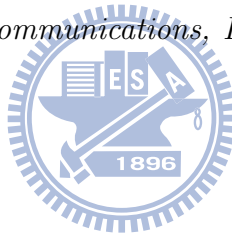


Bibliography

- [1] T. Jiang and Y. Wu, “An overview: Peak-to-average power ratio reduction techniques for OFDM signals,” *Broadcasting, IEEE Transactions on*, Vol. 54, Issue 2, Page(s):257 - 268, June 2008
- [2] A.E. Jones, T.A. Wilkinson and S.K. Barton, “Block coding scheme for reduction of peak to mean envelope power ratio of multicarrier transmission schemes,” *Electron. Lett.*, Vol. 30, Issue 25, Page(s):2098-2099, 8 Dec. 1994.
- [3] A.D.S. Jayalath and C. Tellambura, “Reducing the peak-to-average power ratio of orthogonal frequency division multiplexing signal through bit or symbol interleaving,” *Electron. Lett.*, Vol. 36, Issue 13, Page(s):1161-1163, 22 June 2000.
- [4] B. S. Krongold and D. L. Jones, “PAR reduction in OFDM via active constellation extension,” *Broadcasting, IEEE Transactions on*, Vol.49, No.3, pp.258-268 Sept. 2003.
- [5] S. K. Deng and M. C. Lin, “Recursive clipping and filtering with bounded distortion for PAR reduction,” *Communications, IEEE Transactions on*, Vol.55, No.1, pp.227-230 Jan. 2007.
- [6] S. Janaaththan, C. Kasparis, and B. G. Evans, “A gradient based algorithm for PAPR reduction of OFDM using tone reservation,” *Vehicular Technology Conference, 2008. VTC Spring 2008. IEEE* Page(s):2977 - 2980, 11-14 May 2008

- [7] J. Armstrong, "Peak-to-average power ratio reduction for OFDM by repeated clipping and frequency domain filtering," *Electron. Lett.*, vol.38, pp. 246-247, Feb. 2002.
- [8] J. Tellado and J. M. Cioffi, "PAR reduction in multicarrier transmission systems," *ANSI Document, T1E1.4 Technical Subcommittee*, 2008.
- [9] R.W. Bauml, R.F.H. Fischer, and J.B. Huber "Reducing the peak-to-average power ratio of multicarrier modulation by selected mapping," *Electron. Lett.* Vol. 32, no. 22, pp. 2056-2057, Oct. 1996.
- [10] A.D.S. Jayalath and C. Tellambura, "SLM and PTS peak-power reduction of OFDM signals without side information," *Wireless Comm.* Vol. 4, no. 5, pp. 2006-2013, Sept. 2005.
- [11] E. Alsusa and L. Yang, "Novel redundancy-free and SER-improved selective mapping technique with coded phase sequences for PAPR reduction in OFDM systems," *International Communication Conference 2006. ICC 2006..* Vol. 4, no. 5, pp. 2887-2892, June 2006.
- [12] G. Heidari-Bateni, C.D. McGillem, "Chaotic sequences for spread spectrum: an alternative to PN-sequences," Proceedings of 1992 IEEE International Conference on Selected Topics in Wireless Communication, Vancouver, Canada, pp.437-440, 25-26 June 1992.
- [13] K. Bae, E.J. Powers, "Distribution of envelope power using selected mapping in OFDM systems with nonlinearity," *Acoustics, Speech and Signal Processing, 2008. ICASSP 2008. IEEE International Conference on*, pp.3065-3068, Mar. 31-Apr. 4 2008.
- [14] R.A. Scholtz and L.R. Welch, "Group characters: Sequences with good correlation properties," *IEEE Trans. Inform. Theory* vol. 24, no. 5, pp. 537 - 545, Sep. 1978.

- [15] R. K. Martin and M Haker “*Reduction of peak-to-average power ratio in transform domain communication systems,*” *IEEE trans. Wireless Comm.*, vol.8, no.9, pp.4400-4405, Sept. 2009
- [16] A.D.S. Jayalath, C. Tellambura, “*Peak-to-average power ratio reduction of an OFDM signal using data permutation with embedded side information,*” *Circuits and Systems, 2001. ISCAS 2001. The 2001 IEEE International Symposium on* , vol.4, pp.562-565, 6-9 May 2001
- [17] D. Divsalar, M.K. Simon, “*Trellis coded modulation for 4800-9600 bits/s transmission over a fading mobile satellite channel,*” *Selected Areas in Communications*, vol.5, no.2, pp. 162- 175, Feb. 1987
- [18] D. Divsalar, M.K. Simon, “*The design of trellis coded MPSK for fading channels: performance criteria,*” *Communications, IEEE Transactions on*, vol.36, no.9, pp.1004-1012, Sept. 1988



作者簡歷

董原豪，台北市人，1986 年生

台北市立成功高級中學	2001.09~2004.06
國立交通大學電信工程學系	2004.09~2008.06
國立交通大學電信工程研究所系統組	2008.09~2010.06

Graduate Course:

1. Random Process
2. Digital Signal Processing
3. Digital Communications
4. Coding Theory
5. Information Theory
6. Detection and Estimation Theory
7. Matrix Computations
8. Computer Communication Networks
9. Wireless Communications

